Water Resources Research

RESEARCH ARTICLE
10.1029/2021WR030731

Hydrologic Connectivity and Residence Time Affect the Sediment Trapping Efficiency and Dissolved Oxygen Concentrations of the Atchafalaya River Basin

Daniel E. Kroes[1], Richard H. Day[2], Michael D. Kaller[3], Charles R. Demas[4], William E. Kelso[3], Tiffany Pasco[3], Raynie Harlan[5], and Steven Roberts[6]

[1]U.S. Geological Survey, Lower Mississippi-Gulf Water Science Center, Baton Rouge, LA, USA, [2]U.S. Geological Survey, Wetland and Aquatic Research Center, Lafayette, LA, USA, [3]School of Renewable Natural Resources, LSU Agricultural Center, LSU, Baton Rouge, LA, USA, [4]Retired, U.S. Geological Survey, Baton Rouge, LA, USA, [5]Louisiana Department of Wildlife and Fisheries, Baton Rouge, LA, USA, [6]U.S. Army Corps of Engineers, New Orleans, LA, USA

Abstract Little is known about water movement, volume, or residence time (RT), and how those characteristics affect sediment trapping efficiency (TE) and dissolved oxygen concentrations (DO) in the United States' largest remaining bottomland hardwood swamp, the Atchafalaya River Basin. To better understand these dynamics, this study used bathymetry, lidar, and stage records to determine volumes in the Basin's hydrologically distinct water management units (WMUs). Discharge measurements determined flow distribution and RT. Residence time was compared with DO to identify conditions that coincided with DO increases or decreases. Suspended sediment concentrations (SSC) were used to determine TE relative to calculated and measured discharge and RT. Discharge through units (85–2,200 m^3/s) and RT (0.37–231 d) depended on connectivity and river stage. At high stages, with water temperatures >20°C, DO in the largest WMU declined by −0.21 mg/l/day. DO trends indicated less well-connected areas of the WMU contributed hypoxic waters as the flood wave lengthened and stages fell. In the two WMUs examined for TE, TE (−266% to 99% and up to 38 Gg/day) correlated with hydrologic connectivity, SSC, RT, water volume, and, in one WMU, discharge losses. Long RT and high TE indicated a high potential to process nutrients. These relationships varied among WMUs. Large volumes of sediment-laden water moving over the floodplain combined with long RT, high TE, and hypoxia indicate that this ecosystem has continental-scale importance in reducing nutrient loads to the northern Gulf of Mexico. Reports from other systems suggest similar processes may be operating on other large river floodplains globally.

Plain Language Summary The Atchafalaya Basin is the largest floodplain wetland in the lower United States and the last floodplain interaction of the Mississippi/Atchafalaya River (AR) system before entering the estuaries of the Gulf of Mexico. This study examined the distribution and duration of water on the floodplain of the AR Basin over a range of discharges from normal low water to a normal flood. Large volumes of water moved across the floodplain, carrying and depositing large masses of sediment and nutrients at high flows but exported sediment during low flows. Small inputs of water relative to floodplain volume indicated a high potential to reduce nutrient delivery to the Gulf of Mexico. Oxygen data indicated pockets of poorly connected water were present across the floodplain and contributed to low water oxygen. High water levels on the floodplain could not maintain oxygen levels during the late spring through summer when water temperatures were high. Because of the large amount of flow, sediment, and associated nutrients, the AR Basin is likely important at the continental scale for the reduction of nutrients delivered to the Gulf of Mexico. Reports from other large systems suggest that similar processes are likely occurring on large coastal floodplains around the world.

Key Points:

- Residence times calculated from previous studies of the Atchafalaya River are accurate but do not reflect the conditions on the floodplain of the Atchafalaya River Basin
- Floodplain interactions in the Atchafalaya River Basin are not well represented by main stem river channel sampling
- The Atchafalaya River Basin is likely of continental-scale importance for nutrient trapping

Supporting Information:

Supporting Information may be found in the online version of this article.

Correspondence to:

D. E. Kroes,
dkroes@usgs.gov

Citation:

Kroes, D. E., Day, R. H., Kaller, M. D., Demas, C. R., Kelso, W. E., Pasco, T., et al. (2022). Hydrologic connectivity and residence time affect the sediment trapping efficiency and dissolved oxygen concentrations of the Atchafalaya River Basin. *Water Resources Research*, *58*, e2021WR030731. https://doi.org/10.1029/2021WR030731

Received 2 JUL 2021
Accepted 30 AUG 2022

Author Contributions:

Conceptualization: Daniel E. Kroes
Data curation: Daniel E. Kroes, Michael D. Kaller, Tiffany Pasco, Raynie Harlan, Steven Roberts
Formal analysis: Daniel E. Kroes, Michael D. Kaller, Tiffany Pasco, Raynie Harlan
Funding acquisition: Michael D. Kaller, Charles R. Demas, William E. Kelso, Tiffany Pasco, Steven Roberts

1. Introduction

1.1. Background

Floodplain bottomland hardwood forests provide many valuable ecosystem services, including sediment and nutrient storage and processing, timber production, wildlife habitat, and recreation. All these services are affected in some way by water residence time (RT) and the volume and mass of water, sediment, and nutrients crossing a floodplain. Water RT is the time required to replace a volume of water within a defined area (i.e.) if the volume is

Investigation: Daniel E. Kroes, Richard H. Day, Michael D. Kaller, Charles R. Demas, William E. Kelso, Tiffany Pasco
Methodology: Daniel E. Kroes, Richard H. Day, Michael D. Kaller, Charles R. Demas, William E. Kelso, Tiffany Pasco
Project Administration: Daniel E. Kroes, Michael D. Kaller, Steven Roberts
Resources: William E. Kelso, Tiffany Pasco, Steven Roberts
Supervision: Daniel E. Kroes, Michael D. Kaller
Validation: Michael D. Kaller
Visualization: Daniel E. Kroes
Writing – original draft: Daniel E. Kroes, Richard H. Day
Writing – review & editing: Richard H. Day, Charles R. Demas, William E. Kelso, Tiffany Pasco, Raynie Harlan, Steven Roberts

100 m^3, it is the time for 100 m^3 to enter the area. On a floodplain, water can be lost to evapotranspiration (ET), gained from precipitation (PPT) or diffuse runoff, and have gains or losses from groundwater movement (Doble et al., 2012; Kroes & Brinson, 2004) prior to reentering the river/stream. Residence times have been studied on smaller river floodplains (Helton et al., 2014; Roley et al., 2012; Sullivan et al., 2020) or single lakes on large river floodplains (Bonnet et al., 2008). However, empirical analyses of residence times in large floodplains like the Atchafalaya Basin are uncommon because of the amount of data that must be collected and processed to accurately estimate inputs and volumes (Bonnet et al., 2008) and because there are few intact river/floodplain systems at this scale to study.

The percentage of river discharge crossing a floodplain is highly variable throughout the year, depending on the system. Most large rivers have a period of no or very little discharge across the floodplain (Leopold et al., 1964). Large rivers also exhibit increasing floodplain inundation during the wet season that can last for weeks to months (Kroes et al., 2022; Rudorff et al., 2014a). Anthropogenic influences and hydrogeomorphic variability within river systems also play an important role in flow distribution, with many rivers receiving floodplain discharge primarily as overbank diffuse flow (Hupp et al., 2015; Rudorff et al., 2014b). Rudorff et al. (2014a) found that the average percentage total discharge across the Amazon River floodplain was approximately 0.75%, whereas on the Kafue River, channel constrictions may force 80% of the discharge across the floodplain (Zurbrügg et al., 2012).

Most of the sediment in a fluvial system comes from upstream sources, although autochthonous organic matter deposition, sediment remobilization, and aeolian deposition can also occur (Hupp et al., 2019; Leopold et al., 1964; Wang et al., 2015). During flooding, sediment and nutrients move across the floodplain, and the amount of time water spends on the floodplain (RT) becomes important for nutrient deposition and processing. Longer residence times increase the likelihood of particulate sediment and nutrient deposition and increase dissolved nutrient processing via denitrification, adsorption, and biological uptake (Kroes et al., 2015; Schönbrunner et al., 2012; Scott et al., 2014). However, longer residence on the floodplain can also result in higher water temperatures, widespread hypoxia due to biologic and sediment oxygen demand, and remobilization of deposited C, N, and P, depending on season and RT (Bryant-Mason et al., 2013a, 2013b; Jones et al., 2014; Noe et al., 2013; Pasco et al., 2015; Xu, 2006). Suspended-sediment concentrations on the inundated floodplain can be highly variable depending on several factors, including source availability, timing of floods, timing within the flood wave (Mize et al., 2018), and anthropogenic influences, such as how water control structures are operated (Heath et al., 2015).

Because of their wide floodplains and slow water velocities, rivers on the northern Gulf of Mexico and Atlantic Coastal Plains can trap significant amounts of sediment and nutrients. Small to medium rivers and streams (<340 m^3/s) trap almost all watershed sediment before entering estuaries (Ensign et al., 2014; Kroes et al., 2007; Noe et al., 2016).

Water RT is of particular interest in the Atchafalaya River Basin (ARB) due to its vast size, discharge, the volume of water present on its floodplain, and the potential to reduce nutrient concentrations by particulate sediment deposition and dissolved nutrient processing. This system may also improve the understanding of residence times of similar-sized, unmonitored systems globally. The ARB is the largest and one of the last opportunities in the Mississippi River Delta to reduce nutrient loads by particulate deposition and water column transformations before the water enters the marshes and estuaries of the Gulf of Mexico. The remaining nutrients transported by the Atchafalaya and Mississippi Rivers contribute to the annually occurring "dead zone" in the Gulf (Rabalais & Turner, 2019). Despite the Atchafalaya River (AR) being the fifth largest river in the USA and 45th largest in the world based on discharge (mean 6,530 m^3/sec, USACE, 2022a; USGS, 1987), little is known about water movement and volumes across its floodplain or water RT and how these processes affect sediment trapping and important water quality issues such as dissolved oxygen concentrations (DO).

Hydrodynamic models have been previously developed for the ARB, concentrating on the large, navigationally maintained channel's (river and bypassing channels >100 m^3/s) translation of the flood wave to the floodplain (Moffatt and Nichol, 2012), flow resistance, and water storage (Bell et al., 2018; Jung et al., 2012). Estimates of the relative RT of water in specific areas of the ARB in relation to nutrient processing have been made with deuterium isotopes (Jones et al., 2014). These estimates indicated differences in RT throughout the flood wave between backwater and flow-through areas and indicated a range of river connectivity among floodplain areas.

Large river floodplains like the ARB have the potential to trap teragrams (Tg) of sediment, thousands of metric tons (Mg) of carbon (Hupp et al., 2008, 2019), and hundreds of metric tons of N and P. For example, U.S.

Geological Survey (USGS) samples for sediment and nutrient inputs at the AR at Melville, LA (USGS site #07381495, 2000–2019), indicated that 17% of N and 67% of P entering the ARB are particulate and represent 0.2% and 0.09%, respectively, of the total suspended sediment load (USGS, 2022). However, the potential of floodplains to trap sediment and nutrients is largely limited by their lateral connectivity with the river (Natho et al., 2020).

Litigation by states along the lower Mississippi River and northern Gulf of Mexico coastline seek to change the current regulations that mandate the U.S. Army Corps of Engineers (USACE) operation conditions of the flood control spillways along the Mississippi River that may have detrimental effects on estuarine fisheries (AP, 2020). These lawsuits seek to more frequently utilize upstream flood control features outside of the Mississippi River levees that are now disconnected floodplains. The operation of these features would effectively be a temporary, conditional floodplain restoration like that studied by Kroes et al. (2015) during the 2011 Mississippi River Flood. Studies have found that legacy (prior sediment deposits that are now eroding) and latent nutrient sources within watersheds are limiting the effectiveness of programs aimed at lessening the nutrient delivery of rivers to estuaries (Stackpoole et al., 2021; van Meter et al., 2021). Nutrient reduction studies along other rivers have found benefits to river floodplain reconnections (Natho et al., 2020; Noe & Hupp, 2005). These floodplain reconnection projects offer additional nutrient reductions, however, their ability to trap and process nutrients may be affected by the flow conditions and obstructions to flow across their surface (Kroes et al., 2015; Triantafillou, 2021).

As river/floodplain systems increase in size, the geomorphic and vegetative complexity of the floodplain surface and flow interactions increase (Becker et al., 2018). On some floodplains, like along the Mekong River, structural complexity is being added by agricultural dikes and raised roadways (Fujii et al., 2003). In many large river/floodplain systems like the Congo River Basin, or the Ganges-Brahmaputra River Basin, insufficient in situ monitoring exists to determine the effects of floodplain complexity on water RT on the floodplain or water quality (Becker et al., 2018; Papa et al., 2015; Samanta et al., 2019). On floodplains where in situ monitoring does not exist, researchers have utilized L-Band microwave remote sensing (Becker et al., 2018; Fatras et al., 2021). In the ARB, numerous high-quality streamgages exist that are stage calibrated every two months and collect data at 15 min or daily frequency. On-site discharge measurements made in relation to stage data exist over decades allowing volume and flow distribution analyses as well as how they have changed over time (Kroes et al., 2022; USGS, 2022).

This study investigated the water RT of the ARB and its environmentally and hydrologically distinct water management units (WMU; USACE, 1982) by calculating volumes of water over the inundated floodplain and in open water bodies to compare to measured inputs and outputs at normal river stages and determine water throughput within two of the largest WMUs of the ARB (1.5-year flood to 1.5-year drought; 80% of days 1960–2016, Kroes et al., 2022). The effect of RT was then examined relative to dissolved oxygen (a commonly used and important reactive tracer in previous and ongoing ARB studies; Baustian et al., 2019; Kaller et al., 2011, Kaller et al., 2015; Pasco et al., 2015; Sabo et al., 1999) and suspended sediment trapping efficiency (TE). We hypothesized that: (a) water inputs and residence times would vary significantly among WMU depending on river state and discharge volumes; (b) water RT would influence dissolved oxygen dynamics and the magnitude and duration of floodplain hypoxia; and (c) sediment TE would also vary substantially among river stages and WMU depending on their hydrologic connectivity and water residence times. These analyses provide valuable points of reference regarding flow characteristics of WMUs in the ARB and potential sediment and nutrient removal on the ARB floodplain, creating a framework to assess floodplain restoration projects prior to construction.

1.2. Study Area

The ARB (2,600 km^2) is the largest remaining bottomland hardwood wetland in the United States and the last major floodplain interaction of the Mississippi/AR before entering the modern deltas (Figure 1). There is an established historical record of in situ flow distribution and water level monitoring in the ARB (Kroes et al., 2022; USACE, 2022b; USGS, 2022). Hydrology of the ARB has changed significantly since 1960, resulting in decreased flow distribution to the floodplains (Kroes et al., 2022). The flow into the Atchafalaya from the Mississippi River is regulated by the OId River Control Structure (N31.08°W91.6°) and is mandated by law to approximate 30% of the longitudinal flow (Flood Control Act of 1954, P.L. 780, and 83rd Congress), with 23% coming from the Mississippi River and 7% from the total discharge of the Red River (Heath et al., 2015). Water stages are now much lower during a 1.5-year flood than in 1960, with primary and some secondary distributary

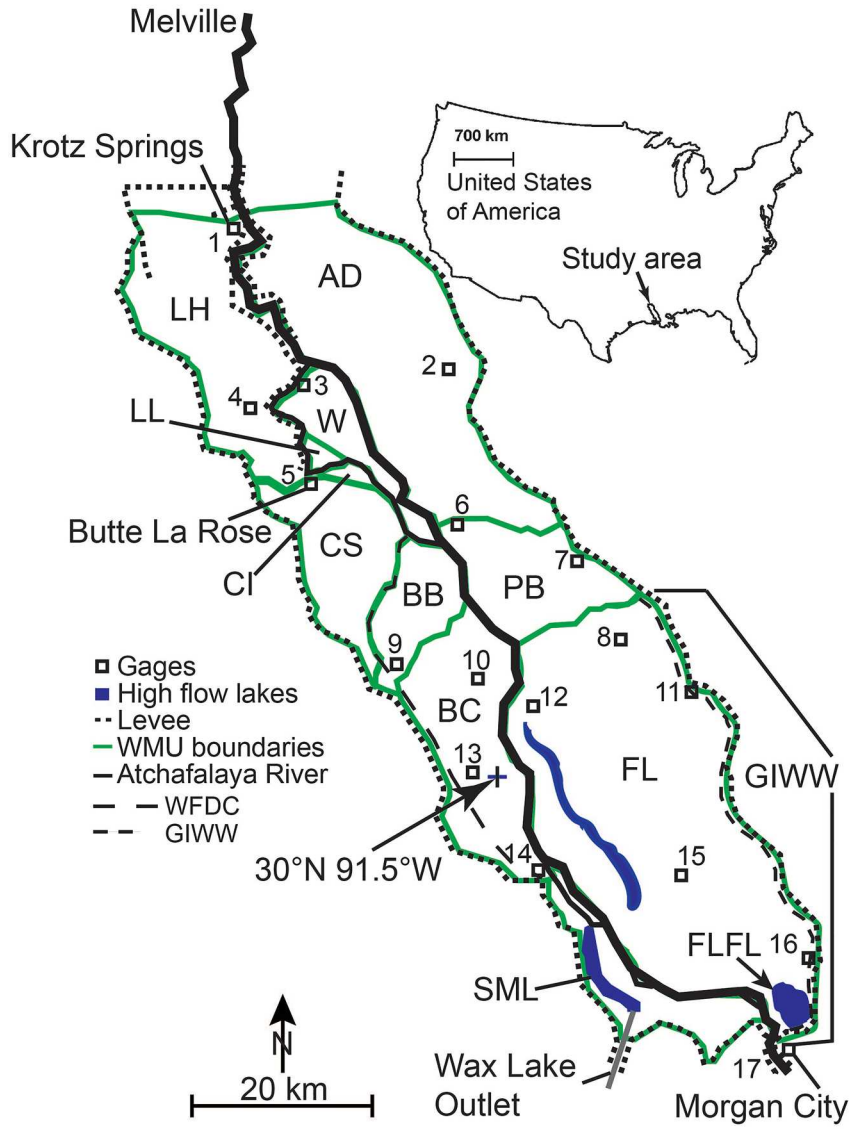

Figure 1. The Atchafalaya River Basin study site. Water management units (WMU) are indicated by letter abbreviations. Streamgages are indicated by numbers. Bypassing channels include Gulf Intracoastal Waterway (GIWW) and West Freshwater Distribution Canal (WFDC). Flat Lake body of FL (FLFL) indicates the Flat Lake portion of the Flat Lake WMU. Lake Henderson (LH), Alabama/Deglaise (AD), Lost Lake (LL), Werner (W), Cow Island (CI), Cocodrie Swamp (CS), Pigeon Bay (PB), Beau Bayou (BB), Buffalo Cove (BC), Flat Lake/Upper Belle River (FL), and Six Mile Lake (SML). Base maps modified from Kroes and Brinson (2004) and USACE (1982).

banks above normal flood water elevations (Kroes et al., 2015, 2022). As a result of these high banks, most water inputs and outputs to WMUs are channelized up to the stage of a 1.5-year flood. Analyses of remote sensing imagery of ARB turbidity within WMUs (USACE, 1982) indicated a range from high to low hydrologic river connectivity. Well-connected units exhibited widespread and large inputs of river water. Poorly connected units exhibited limited inputs and outputs (Allen et al., 2008). Some units had singular input and ouput (I/O units) that received water from the river via one channel and drained through the same channel. Rising and falling stages of the river often resulted in a range of stages within the WMUs because of large storage capacities and a limited ability to drain.

The 2,200 km^2 area examined in this study is within the ARB Protection levees and includes areas that would be inundated in a 1.5-year flood (4.8 m) as determined at the USGS Butte La Rose (BLR) streamgage (USGS site #07381515, Kroes et al., 2022). The 127-km reach of river examined was from Krotz Springs (KS) to Morgan

Table 1
Streamgages Used for Analyses and the Associated Water Management Units (WMU)

Streamgage # on Figure 1	Streamgage station number	Operator	Correction: Stage to NAVD88 (m)	WMU water surface
1	03075	USACE	−0.04	R
2	49415	USACE	0	A, D
3	03240	USACE	−0.17	R
4	302020091435700	USGS	0	LH
5	07381515	USGS	−0.28	LL, W, CI, CS
6	03315	USACE	−0.27	D
7	49570	USACE	−0.19	PB, D
8	073815963	USGS	−2.12	FL
9	300507091355600	USGS	−1.98	CS, BB
10	300312091320000	USGS	−0.61	BC
11	49630	USACE	−0.37	PB
12	03615	USACE	−0.28	FL, FL(B)
13	07381567	USGS	−0.21	BC
14	073815450	USGS	−0.16	R, BC, SML
15	295447091191500	USGS	−0.15	FL (B)
16	49725	USACE	−0.27	FL (B)
17	07381600	USGS	−0.39	R

Note. R = River, A = Alabama, D = Deglaise, LH = Lake Henderson, LL = Lost Lake, W = Werner, CI = Cow Island, CS = Cocodrie Swamp, PB = Pigeon Bay, FL = Flat Lake, FL(B) = Upper Belle River portion of Flat Lake, BB = Beau Bayou, BC = Buffalo Cove, SML = Six Mile Lake (USACE, 2022b; USGS, 2022).

City (MC), Louisiana (Figure 1). The Alabama Bayou and Bayou Deglaise WMUs defined by the USACE (1982) were combined into AD, and the Flat Lake and Upper Belle River Units were combined into FL. This combination provided AD and FL with distinct inputs from major waterways and outputs to major waterways.

Annual air temperature in the ARB averages 20.1°C (1981–2010), with an average annual PPT of 152 cm (U.S. Climate Data, 2022). Mean discharge of the AR from 1984 to 2011 was 6,530 m^3/s measured by the U.S. Army Corps of Engineers streamgage #03045 at Simmesport, LA (USACE, 2022a). Water temperature on the floodplain commonly exceeds 30°C during summer months, and hypoxia is widespread on the inundated floodplain from late spring to early fall (Kaller et al., 2011; Pasco et al., 2015). Forested portions of the floodplain can experience annual hydroperiods of more than 270 days or longer in areas with local impediments to drainage (Kroes et al., 2022).

Vegetation in the ARB is typical of a bottomland hardwood swamp in the northern Basin grading to cypress (Taxodium distichum *Richard.*)/tupelo (Nyssa aquatica *L.*) swamps mid-basin with a button bush (Cephalanthus occidentalis *L.*), red elm (Ulmus rubra *Muhl.*), and privet (Ligustrum sp.) understory. Higher elevation floodplains and levees may have dense herbaceous undergrowth, including Poeaceae, Cyperacea, Juncaceae, and Rubus sp. grading to Peltandra sp. or unvegetated swamp floor. Areas of low-velocity water may have substantial, year-round coverage by invasive species like Salvinia sp. and/or Pontederia crassipes *Mart*. (Piazza, 2014).

2. Methods

2.1. Water Volumes

Water volumes were calculated by determining water surface elevations, open water area, bed elevations, and floodplain surface elevations. Federal, state, and local entities regard stages at BLR to be a good representation of water surface elevation and flow conditions through most of the ARB (Allen et al., 2008). Water elevations of the river for the sampled BLR stages were determined for rising and falling limbs of the hydrograph during synoptic discharge missions in the combined Flat Lake and Upper Belle River units (hereafter FL, Figure 1). The sampling missions with the closest BLR stage as FL were selected for the Buffalo Cove (BC) WMU comparison, ranging from 0.91 m (tidal, 1.5-year drought) to 4.8 m (1.5-year flood; Kroes et al., 2022). Water levels within the units were calculated from stages recorded by USGS and USACE streamgages corrected to NAVD88 elevation (Table 1, Figure 2). If no streamgages were available within a unit, the closest streamgage representative of water levels inside the WMU was used. In many cases, stages were not available on an exact date due to streamgage malfunctions, stage errors, and lapses in record. In these cases, an alternate date that met the same BLR stage date and hydrograph position was selected (Table 2). In the combined units (AD and FL), water surface elevations and volumes were calculated for the individual units and then combined. Water levels within the units were calculated as a flat surface within the WMUs.

The ARB has thousands of kilometers of permanent lakes and channels (natural and dredged). Open water (lakes and a subset of channels off the main channel) was identified by a modified National Hydrography Database (NHD) set coverage of waterbodies (USGS, 2011). These waterbodies were surveyed at high water from 2014 to 2017 with a SONAR chart plotter (±0.1 m), with water surface elevations measured at both ends of the surveyed reach with real time kinematic survey-grade elevational GPS equipment. These SONAR data were used to calculate mean bottom elevation for lakes and reaches of channels (Kroes, 2022). Reaches of the channel were determined by observed and defined changes in bottom elevation. In nonsurveyed channels, mean depth was estimated by averaging the mean bottom elevations of similar, measured channel types located within 4 km as determined by field reconnaissance and visual comparison of imagery available on Google Earth (2019). Of the open water bodies, not including the main river channel, 68% were cross-section surveyed, 16% were estimated

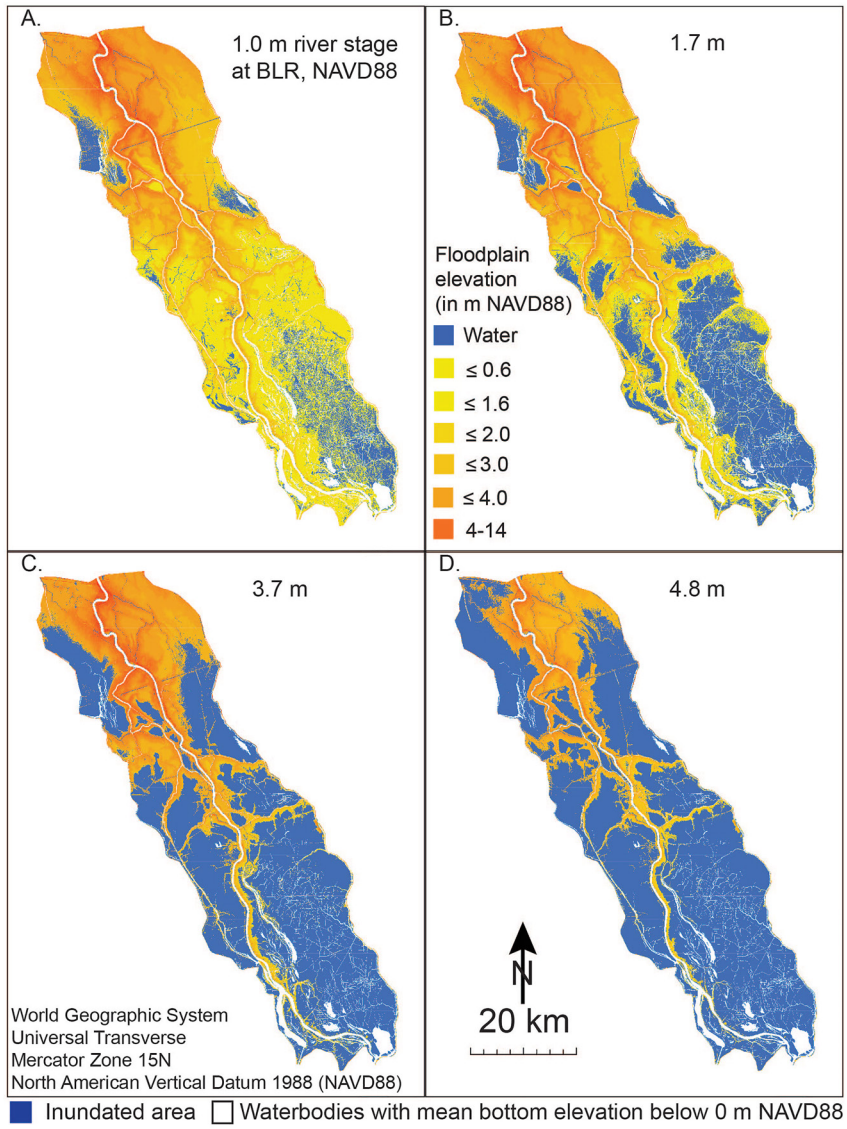

Figure 2. Lidar-derived elevation maps of the Atchafalaya River Basin (USGS, 2014a). Blue indicates inundation at the examined Butte La Rose (BLR) stages and the corresponding mean water levels calculated for each water management units (WMU) for the (Table 1 and Table S1 in Supporting Information S1). White indicates elevations below 0 m NAVD88.

by imagery, 10% were estimated from nearby waterbodies, and 6% had surveyed elements within a larger NHD waterbody (Kroes, 2022). Surface areas of these waterbodies were calculated with the 3D Analyst tool of ArcPro (ESRI, 2019).

A mean bottom-elevation shapefile was developed for the study of water bodies and combined with the 2012, 1 m lidar (Kroes, 2022; USGS, 2014a) and water surface elevations, as determined above, to calculate the volume of water above the floodplain and waterbody beds for the WMUs at each NAVD88 rising or falling stage elevation with the 3D Analyst tool of ArcPro (ESRI, 2019). The 2012 lidar was flown at a BLR stage 0.6 m lower than the 2010 lidar (USGS, 2011), gaining floodplain surface definition for hundreds of km^2 of the lower ARB. Main river channel volume was removed from this analysis and calculated separately. Where there was a difference in WMU stages for rising and falling stages of the river due to the ability of a unit to drain or fill, the volume used for RT was the mean volume of the rising and falling stages. In WMUs that included large bypassing channels—such as the Gulf Intracoastal Waterway (GIWW), the West Freshwater Distribution Canal (WFDC, Kroes et al., 2022), and other large WMU border channels—volume of the WMU was calculated with and without the bypassing channel to calculate the internal volume and to calculate the entire WMU volume. For bypassing channels that

Table 2
Stages and Alternate Dates Examined for Water Surface Elevations

Stage (m NAVD88)	Hydrograph limb	Dates examined for WMU stages (dd/mm/yr)
0.91	Tidal	11/09/12; 19/11/16
0.99	Tidal	15/11/10; 19/11/16
1.68	Rising	28/02/11; 30/12/16; 26/01/18; 28/09/19
1.68	Falling	10/09/10; 22/08/11; 11/07/16; 18/09/19
3.51	Rising	13/04/05; 07/03/11; 30/01/17; 31/10/19
3.51	Falling	10/07/13; 16/06/16; 17/08/19
3.67	Rising	11/05/10; 08/03/11; 14/04/17; 02/11/19
3.67	Falling	05/07/13; 12/06/16; 08/17/19
3.81	Rising	08/03/11; 09/03/11; 16/04/17; 13/12/19
3.81	Falling	04/07/13; 03/05/16; 16/08/19
3.96	Rising	10/03/11; 20/04/17; 12/11/18; 30/12/19
3.96	Falling	21/04/10; 30/04/16
4.75	Rising	30/03/11; 13/05/17; 15/11/18; 02/01/19; 18/01/20
4.75	Falling	01/06/13; 09/08/19
4.82	Rising	01/04/11; 17/05/13; 05/01/16; 04/01/19; 19/01/20
4.82	Falling	06/04/16; 07/08/19

Note. Alternate dates were examined for each stage due to streamgage errors or missing data.

form the boundary between WMUs, half of the channel volume and discharge were considered in analyses for the adjacent WMUs.

The volume of the main channel was calculated from the 2010 multibeam SONAR hydrographic survey conducted by the USACE (USACE, 2012). The reach of river was subdivided between main channel streamgages and then divided further into 19 variable length sections that had less than 0.3 m difference in surface elevation between the upstream and downstream ends at a BLR stage of 4.8 m, assuming steady slope between streamgages 1, 3, 14, and 17 (Figure 1, Table 1).

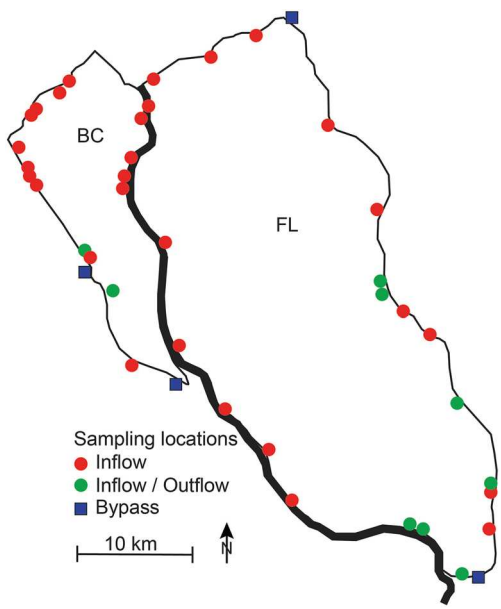

Figure 3. Discharge and suspended sediment sampling locations around FL and BC water management units (WMUs). Basemap modified from USACE (1982).

2.2. Discharge Measurements/Estimates

FL and BC WMUs were previously identified (Allen et al., 2008) as being well-connected units with numerous inputs and outputs, whereas other units had minor floodplain discharge or area. Measurements were made in coordinated synoptic discharge missions for these largest high connectivity WMUs; BC (n = 26, 2003–2018; USGS, 2022) and FL (n = 6, 2010–2011; USGS, 2012) with standard USGS moving-boat acoustic DOPPLER current profiler techniques (Simpson, 2001) at almost all channel inputs and outputs (Figure 3). For these measurements, the tolerance of variation within a measurement was designated to be acceptable if $\leq \pm 5\%$ discharge variation was observed between a minimum of four repeated transects in paired left/right bank starting sequences. Sampling dates for BC were selected that closely matched the BLR stages sampled for FL.

Previous discharge measurements in 4 channels of similar width in the BC unit as the input channels to CS and AD exhibited a mean 1.5-year flood discharge of 50 m^3/s ($\pm 7\%$ around the mean) (USGS, 2022). Hydraulic gradients in the ARB are flat (Kroes et al., 2022) and field observations indicate the bank and bed materials along secondary distributaries to generally be fine sand to clay. For the CS and AD WMUs that had unmeasured incoming

discharge, estimates were made based on observations of discharge and comparison with a measured channel of similar dimensions [AD: Work Canal, width 29 m, N30.250° W91.534°; CS: Borrow Pit Canal, width 40 m, N30.219° W91.692° (Poncho Chute width 39 m, N29.976° W91.520°, pre-2016) with a stage/discharge regression equation of $Q = -229.4 + 150.6x + 82.54x^2$, where x = stage (m) at BLR]. Discharge within the AR channel was the calculated discharge from the USGS/USACE Simmesport streamgage (USGS site #07381490). For WMUs that bordered the GIWW and the WFDC channels, the amount of discharge going to the interiors of the units as well as the discharge bypassing the units were measured. For WMUs that had singular I/O channels, no estimates were made for discharge. Precipitation was an episodic input and was considered separately. Gains in discharge through a WMU were positive, losses were considered negative.

2.3. Precipitation/Evapotranspiration Estimates

Meteorological data were not available within the study area, so ET was calculated from solar radiation, daily mean temperature, and humidity at the nearest agricultural monitoring station (2001–2011, Jeanerette, LA; LAIS, 2022). ET was calculated with the Turc ET model (Fontenot, 2004; Turc, 1961). Missing day data for ET were estimated as the mean of the adjacent days. Missing days of PPT record were not identified in the data set, so if they occurred, they were considered to be zero PPT. Data to calculate ET and PPT were collected at this station from September 2001 to June 2011.

Comparison of daily ET and PPT was beyond the scope of this project. The mean annual ET and PPT were calculated and divided by 365 to determine a mean daily ET and PPT. Mean daily ET was subtracted from the daily PPT to determine the daily PPT exceeding the ET (ex-PPT). The percentage exceedance was calculated for daily ex-PPT (Figure S1 in Supporting Information S1). The volume of the ex-PPT was calculated based on the total WMU areas with bypassing channels and the river channel removed, as well as the whole study area multiplied by the ex-PPT values for the mean, 10%, 1%, and 0% exceedance. Median PPT was not used because it was zero. This volume was then calculated as a ratio of ex-PPT to ARB and WMU volumes at stage. Neither runoff rates from the contributing WMU areas nor soil and vegetation moisture deficit water uptakes were considered beyond the mean ET values. One-hundred percent ex-PPT runoff was assumed.

2.4. Groundwater Estimates

Groundwater inputs or outputs could influence the amount of water flowing through WMUs (Joung et al., 2019). However, insufficient data existed to quantify groundwater movement either within this area or surrounding areas. Losses or gains to groundwater were calculated as the difference between the total WMU inflows and outflows.

2.5. Residence Time Calculations

Residence times for WMUs with throughflow were calculated as the time required for inflowing discharges to equal the volume of water within a WMU at a given stage. For RT calculations, only the water inputs by channel were considered. Rather than using a throughput estimate for singular I/O WMUs, RT was determined based on the stage exceedance curve for the AR at BLR for 2000–2009 (Kroes et al., 2022, Figure 4a). Days where water was above stage X were determined by multiplying the percent exceedance by 365 days. Residence time was only calculated for days above the I/O channel bed elevation as determined by bathymetry or lidar-determined elevations. Residence time was not calculated in these units for water elevations that could not drain by surficial channels. Lake Henderson WMU was removed from this study of RT because it has a singular AR-sourced I/O but also had an external flood-control-driven input that was large (≈100 m^3/s), irregularly timed, and unmonitored for discharge.

Residence time of the entire ARB was calculated based on the residence times of each unit, bypassing channels, and the river channel RT for the investigated stages. Residence time of each was multiplied by the water volume of the unit or waterbody and totaled. These weighted values were then divided by the entire calculated water volume of the ARB, which created a volume-weighted RT for each investigated stage. No attempt was made to determine the RT for water that could not drain due to topographic or biogenic barriers to flow within each unit except where the I/O channel bed was the barrier.

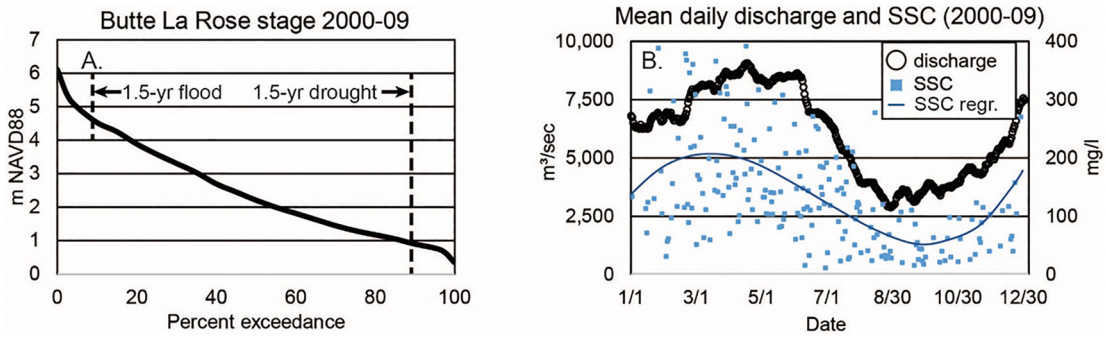

Figure 4. Atchafalaya River Stage percent exceedance at Butte La Rose (a) and mean daily discharge, suspended sediment concentration, and the regression line of suspended sediment concentrations (SSC) (b) for the 10-year Period 2000–2009. The 1.5-year flood and drought exceedance are indicated in panel (a) at 10% and 90% exceedance (Kroes et al., 2022).

2.6. Dissolved Oxygen

The relationship between RT and floodplain dissolved oxygen (DO) levels was examined in FL, which had the longer time series of measurements of the two WMUs (39 observations in BC vs. 217 observations in FL meeting criteria below). We limited our analyses to the latter stages of the annual flood pulse, based on results of previous research indicating widespread floodplain inundation at 3.7 m at BLR (USGS site #07381515), and a strong association of low dissolved oxygen levels with water temperatures ≥20°C (Kaller et al., 2011; Pasco et al., 2015). DO was measured in situ using Yellow Springs Instruments or Hydrolab sondes calibrated at least weekly. For all flood years, mean floodplain DO levels across sites per day (when water temperatures were ≥20°C) were plotted against the days at BLR stage heights of 3.7, 4.0, and 4.7 m, and were analyzed with generalized linear mixed models (GLMs; Kaller, 2022; identity link with normal distribution, log link with lognormal distribution, log link with exponential distribution, log link with Poisson distribution, and inverse link with Gamma distribution). Candidate models were evaluated for model fit by the Pearson X^2/degree of freedom fit statistic, root mean square error (RSME), and the mean absolute error (MAE), and the best-fitting version was selected for analyses. Each GLM included RT (in days) at the three river stages of interest as fixed explanatory variables, flood year as a first-order autoregressive random variable, and dissolved oxygen concentration as the response variable (PROC GLIMMIX, SAS vers.9.4, SAS Institute, Inc., Cary, NC).

2.7. Sediment Trapping

Sediment TE was calculated by mass for the interiors of the FL and BC WMUs based on the volume of water and concentration of sediment entering and leaving the unit. Depth-and flow-integrated suspended sediment samples (SSC) were collected during synoptic discharge measurements in FL and BC WMUs with the multiple vertical method, incorporating weighted bottle and bag type flow integrated samplers (Figure 3). A US DH-2A bag-type sampler was used where mean water velocity exceeded 0.6 m/s, the velocity at which samplers are calibrated to collect isokinetic samples. Below this velocity, weighted bottle samplers were used (depth-integrated grab-sample, Davis, 2005; Guy & Norman, 1970). Samples were collected for FL from April 2010 to April 2011. Samples for BC synoptic discharge sets were collected by USGS from September 2015 to April 2018. For BC discharge measurements prior to those dates, incoming SSC was estimated from USACE sampling at primary distributary locations (January–June) or USGS samples taken from the AR at MC (USGS site #07381600) on the date closest to the discharge measurement date (USGS, 2022). Outflowing water from BC was typically low-SSC blackwater. Where no similar samples existed (1.68 and 3.51 m BLR), outflowing waters from BC were considered to have the same SSC as the mean of the other sampling dates.

Samples were collected for one large bypassing channel (GIWW) at the same time as the FL measurements. The total daily trapping at similar stages of FL and GIWW was compared with the daily AR load input at Melville, LA (USGS site #07381495), and river output total of Wax Lake (USGS site #07381595) and MC based on the SSC of the closest sampling date to the FL sampling dates (USGS, 2022). For BC, the percentage of river load trapping was calculated based on measured water inputs at a specified stage and sediment trapping efficiencies at that stage multiplied by the River SSC for the same dates as FL. The percentage of river sediment load

trapping was the sum of the sampled FL, and GIWW, and BC trapping divided by the total river load. To aid in the interpretation of the results, the Flat Lake body of FL (FLFL) inputs and outputs were also examined. Total annual sediment trapping (mass) rates were not estimated. Although the WFDC is a similarly large, depositional, bypassing channel adjacent to BC, insufficient data existed to make estimates of sediment storage within the channel. Net sediment trapping in a WMU was indicated as positive, and net sediment export was indicated as negative trapping.

3. Results

3.1. Distribution of Water Volumes

For the same BLR stage, AD exhibited the largest range of stages (0.76 m) at streamgages during a 1.5-year flood, although streamgages physically within AD exhibited a smaller range (0.53 m). The largest WMUs exhibited a much smaller range of stages between the upstream and downstream gages (stage range: BC = 0.25 m and FL = 0.18 m). Stages during rising and falling limbs of the hydrograph exhibited a range in stage of up to 0.59 m at gage #13 (Figure 1, Table 1). However, most streamgages showed less than 0.3 m in range from falling to rising limbs of the hydrograph. In BC, the maximum single streamgage difference (0.59 m at 3.66 m at BLR) between the rising and falling stage resulted in a WMU stage range of 2.18–2.56 m. This range in stage resulted in a volume range of ±14% around the mean at 3.66 m BLR.

Water volume distribution of the ARB varied with the stage of the river. The total water volume for the stages examined in this study ranged from 980 to 3,040 ha^3. During low water stages (BLR stage of 0.91 m), the river channel contained 65% of the total volume of the ARB. As stages rose, the percentage of water in the river channel declined to 27% at 1.5-year flood stage (4.8 m BLR). Units with high connectivity (FL, BC, and SML) contained from 30% (low stage) to 50% (high stage) of the water in the ARB. Units with limited connectivity (AD and CS) represented from 3% to 13% over the range of river stages. Singular I/O units contained from 2% to 10% of the volume (Figures 5 and 6, Tables S1, S2, and S3 in Supporting Information S1).

3.2. Flow Distribution

Inflowing river discharge ranged from 1,600 to 12,000 m^3/s (Figure 7). The mean percentage of discharge passing through SML for sampled stages was 54% (3,540 m^3/s) of the ARB discharge, while discharge through the remaining units ranged from 85 to 2,200 m^3/s, with the greatest percentage of off-channel discharge moving into FL and BC. Discharge into FL ranged from 4.8% to 12%, averaged 8.3% of the total ARB discharge for sampled stages, and was highly variable. This variability may have been in part due to the influence of FLFL hydrology, that may have been influenced by Gulf of Mexico water levels (seiches). Seiches along the northern Gulf Coast typically occur when strong winds (hurricanes, tropical disturbances, or broad fronts) blow from the south or in a direction that forces water into a bay or estuary, resulting in temporarily higher water levels. These higher water levels in the Gulf can temporarily reduce outflows from the AR and units closer to the Gulf like FLFL and other outflows from FL by increasing water storage. Lower Gulf levels, caused by winds blowing from the north, would increase outflow, by reducing water storage. Discharge into BC ranged from 0.2% to 3.7%, with a mean sampled input of 1.5% of the total ARB discharge. Poorly connected units (AD and CS combined) had a mean discharge equal to 0.98% of the total (Figure 7). The combined filling discharge of the singular I/O units (BB, PB, LL, W, and CI) could equate to 88 m^3/s (1.3% mean of sampled river discharges) if these units filled over a 100-day period. It should be noted that the percentages of WMU inflow are not directly comparable with the flow off-river presented in Kroes et al. (2022). Discharge into FL includes multiple large inputs and outputs of several hundred m^3/sec into and out of the bypassing channel that enter the interior of the unit (intrafloodplain flow patterns) but were not included in the Kroes et al. (2022) analysis of distribution out of the river to the floodplain.

3.3. Water Balance

Lidar data (USGS, 2014a) in relation to water levels indicated that WMU edge boundaries were above water at a BLR stage of 4.8 m, except for the downstream boundaries of BC and WFDC (19% of length) and the downstream boundary of FL and GIWW (21% of length). Flow observations and elevational patterns on these submerged margins indicated that water in these areas had minor discharge into the bypassing channels at the

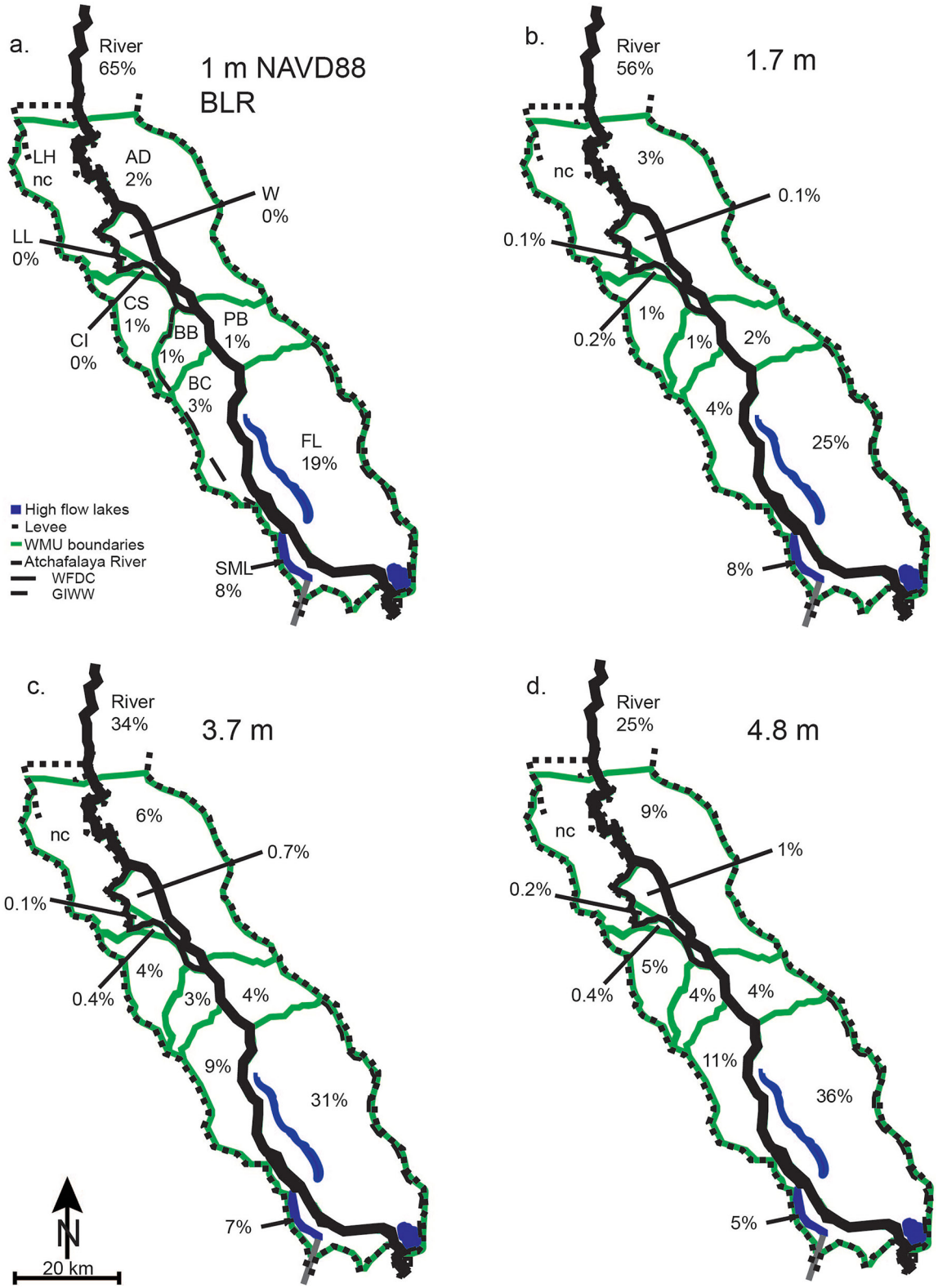

Figure 5.

10.1029/2021WR030731

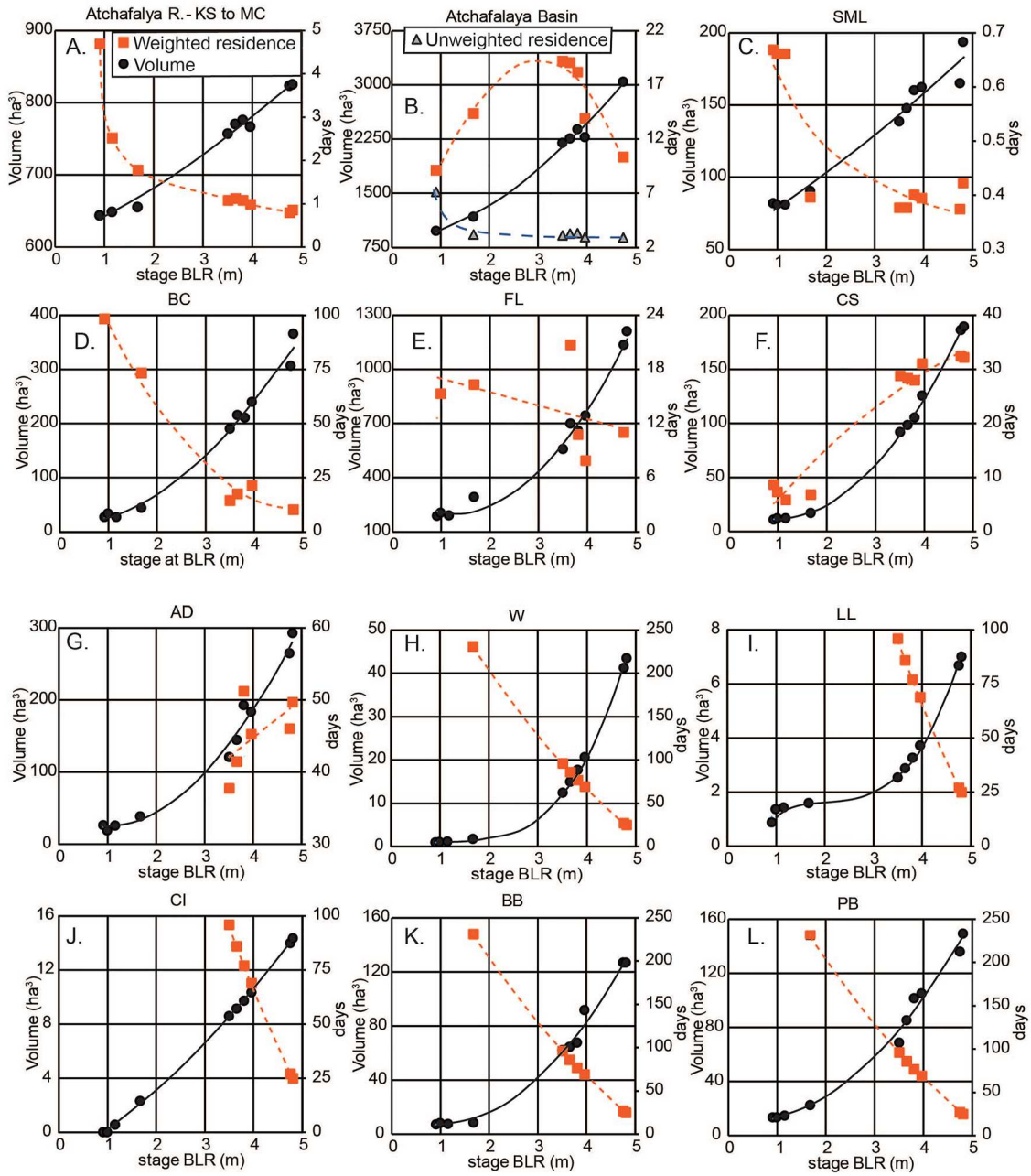

Figure 6. Residence time (RT) and water volume of the River (a), the Atchafalaya River Basin (ARB) (b), and the water management units (WMUs) (C–L). The ARB (b) includes the RT weighted and unweighted by volume of individual WMUs. WMUs include the RT of included bypassing channels, weighted by volume. AD = Alabama/Deglaise, LL = Lost Lake, W=Werner, CI=Cow Island, CS=Cocodrie Swamp, BB=Beau Bayou, PB=Pigeon Bay, BC=Buffalo Cove, FL=Flat Lake, and SML=Six Mile Lake.

stages investigated here (Figures 2c and 2d). Because the boundaries were above water elevations, inputs and outputs from surface water were well represented by channel discharge (Table 3).

Figure 5. Percentage of the Atchafalaya River Basin water volume contained within the water management units (WMU) and the river channel. Volumes were examined for a range of stages at Butte La Rose (BLR), representing the 1.5-year flood to 1.5-year drought. A 0% volume indicates an insufficient volume to be represented in this figure and does not indicate that water is absent. In most cases water is held in those units above low river stages. LH = Lake Henderson, AD = Alabama/Deglaise, LL = Lost Lake, W=Werner, CI=Cow Island, CS=Cocodrie Swamp, BB=Beau Bayou, PB=Pigeon Bay, BC=Buffalo Cove, FL=Flat Lake, SML=Six Mile Lake, WFDC=West Freshwater Distribution Canal, GIWW = Gulf Intracoastal Waterway, NAVD88 = North American Vertical Datum of 1988, and nc = not calculated. Base map modified from USACE (1982).

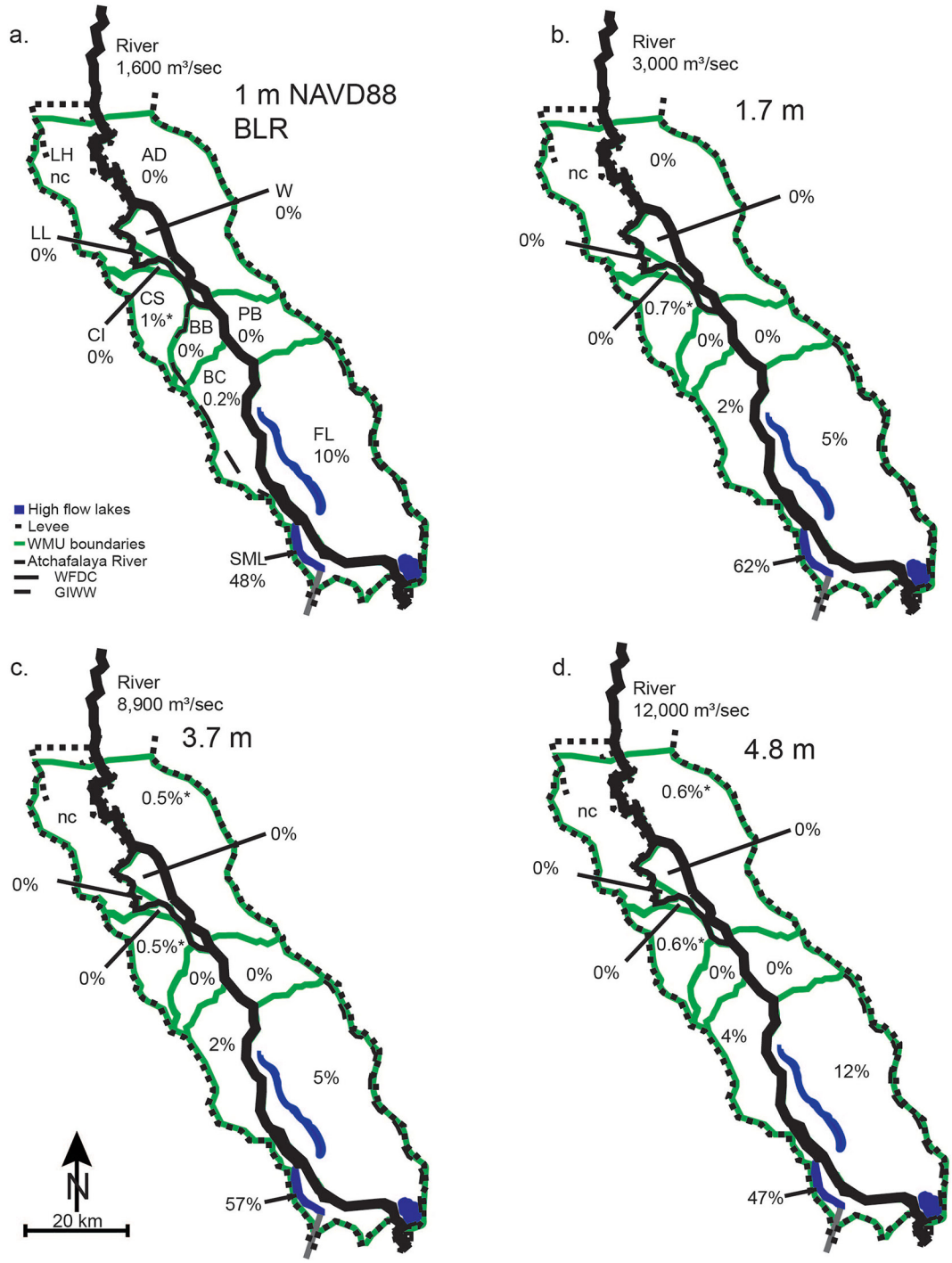

Figure 7. Percentage of river discharge entering water management units (WMU) of the Atchafalaya River Basin excluding bypassing channels. Discharge distribution was examined for a range of stages at Butte La Rose (BLR) representing the 1.5-year flood to 1.5-year drought before 2015. Incoming river discharge is indicated for each panel. A 0% distribution indicates too little flow to be represented in this figure and does not indicate zero discharge. Discharge was estimated (*) for CS and higher stages of AD. LH = Lake Henderson, AD = Alabama/Deglaise, LL = Lost Lake, W=Werner, CI=Cow Island, CS=Cocodrie Swamp, BB=Beau Bayou, PB=Pigeon Bay, BC=Buffalo Cove, FL=Flat Lake, SML=Six Mile Lake, WFDC=West Freshwater Distribution Canal, GIWW = Gulf Intracoastal Waterway, NAVD88 = North American Vertical Datum of 1988, and nc = not calculated. Base map modified from USACE (1982).

Table 3
Inputs and Outputs of Water and Sediment to FL and BC WMUs, and Bypassing Channels GIWW and WFDC

	Sample date (dd/mm/yr)		Input m^3/sec (mean SSC mg/l)					Output m^3/sec (mean SSC mg/l)				
BLR stage	FL, FLFL GIWW	BC	FL	FLFL	GIWW	BC	WFDC	FL	FLFL	GIWW	BC	WFDC
0.91		11/09/12				3.2(36*)	58				1.4(36*)	69
0.99	15/11/10		154(112)	83(75)	243(53)			398(69)	291(72)	292(88)		
1.68	10/09/10	28/07/09	206(72)	183(11)	278(81)	7(95*)	185	514(77)	419(36)	336(58)	18(27*)	153
3.51		13/04/05				151(227*)	266				35(27*)	376
3.66	11/05/10	14/03/05	391(108)	249(79)	504(71)	142(116*)	326	481(47)	311(17)	375(66)	44(21*)	367
3.81	08/03/11		710(445)	393(108)	451(502)			403(74)	356(77)	465(225)		
3.96	21/04/10	18/04/17	1090(138)	554(106)	790(117)	130(189)	542	1044(49)	821(51)	766(128)	7.4(21)	579
4.75	04/04/11		1190(179)	697(67)	702(129)			1190(47)	934(35)	829(105)		
4.82		06/04/16				414(94)	715				18(28)	816

Note. Mean SSC (in parenthesis) is weighted by discharge. Sampling dates are the middle of sampling mission with duration up to a week. * Indicates SSC was estimated from USACE and USGS data from nearby sampling locations during similar conditions and dates. WFDC did not have SSC data.

Evapotranspiration was calculated to have a mean annual total of 449 mm and a mean daily value of 1.23 mm. Precipitation at the Jeanerette monitoring station was found to have a mean annual total of 138 cm over the same time. Examination of the PPT record indicated 66% of days had no PPT and an additional 11% of days did not exceed the mean daily ET. The mean daily ex-PPT was 2.54 mm. Analysis of the ex-PPT exceedance curve indicated 9.18 mm ex-PPT had 10% exceedance, 55.4 mm–1%, and 200 mm–0% was the maximum observed (Figure S1 in Supporting Information S1).

These ex-PPT amounts, when applied to the entire 2,200 km^2 study area, total 5.63, 20.4, 123, and 444 ha^3 of water (Table S4 in Supporting Information S1). Exceedance less than 10% was not investigated in this study but the 1% and 0% ex-PPT exceedance did result in a substantial input to the Basin, representing from 13% to 45%, respectively of the ARB water volume at a 1.5-year drought stage. At 1.5-year flood stage, these ex-PPT amounts were from 3.7% to 13% of the ARB volume (Table S4 in Supporting Information S1). For I/O units (LL, W, CI, CS, BB, and PB), the mean and 10% ex-PPT (2.54 and 9.18 mm) was a substantial water input at 1.5-year drought stages of BLR, particularly at stages below the level of channel obstructions. Similarly, in CS and AD, a 10% ex-PPT exceedance resulted in a 11%–16% input of water at lower stages. At stages above 3.5 m BLR, a 10% ex-PPT rainfall resulted in less than a 6% input of water for all WMUs. In the same scenario, FL, BC, SML, CS, BB, and CI saw less than a 2% ex-PPT input of water (Table S4 in Supporting Information S1).

FL generally gained discharge (greater surficial channel output than surficial input) at lower stages; the FLFL portion of the unit was a major source of discharge gains, and gains were greater at lower river stages (Tables 3 and 4). It was unclear if the source of gain was from wind seiche, tidal flux, or groundwater inputs. When FLFL discharge gains are removed from the FL water balance, the unit gained 35% discharge relative to inputs at the lowest sampled stage. This gain may have been due to a rapidly dropping river stage, limiting inflows while enhancing outflows.

At higher stages, FL minus FLFL lost up to 43% of discharge. Discharge losses at high stages were large (−29%) during falling limb sampling dates of the river hydrograph (3.96 m BLR). These losses may not have been measured by channelized discharge but also may not be due to water storage within the unit or groundwater losses. Unmeasured discharge losses contributed from FL into FLFL were likely unchannelized sheet flow at higher stages when the margin between the two areas became submerged. Aerial imagery supports the idea that sheet flow between FL and FLFL does occur Google Earth, 2019. Discharge gains or losses within FL did not correlate with gains or losses in the bypassing channel (GIWW, $R^2 < 0.001$) or the river ($R^2 < 0.001$).

Discharge losses were substantial in the BC unit and increased with river stage (Tables 3 and 4). During all USGS synoptic missions, only 3 of 26 missions through the hydrograph showed greater or equal outflow from the unit than inflow (USGS, 2022). One sampled stage (1.68 m, Table 3) showed a 11 m^3/s gain in discharge through the WMU. This sample date was preceded by a 29.8 mm ex-PPT event at the Jeanerette station (LAIS, 2022) with a

Table 4
Calculated Discharge and Sediment Balances and Percentage of Sediment Export of the FL and BC WMUs and Bypassing Channels GIWW and WFDC

	Discharge m^3/sec, gain or (loss)						Sediment trapping Gg/day, storage or (export)					% of sediment input leaving WMU			
BLR stage	FL	FLFL	FL-FLFL	GIWW	BC	WFDC	FL	FLFL	FL-FLFL	GIWW	BC	FL	FLFL	GIWW	BC
0.91					(1.8)	11					0.01				42
0.99	244	208	36	49			(0.9)	(1.3)	(0.39)	(1.1)		160	335	197	
1.68	308	236	72	58	11	(32)	(2.1)	(1.1)	(1.0)	2.6	0.02	266	320	87	75
3.51					(116)	110					2.3				3
3.66	90	62	28	(129)	(98)	41	1.7	1.2	0.45	0.95	1.3	53	84	69	6
3.81	(307)	(37)	(270)	14			25	1.3	23	11		9	64	46	
3.96	(46)	267	(313)	(24)	(123)	36	8.6	1.5	7.1	(0.5)	2.1	35	71	133	1
4.75	0	237	(237)	127			14	1.2	12	0.3		25	70	96	
4.82					(396)	101					3.3				1

Note. Sediment balance and the percentage of sediment export were not calculated for WFDC. Gigagrams (Gg). Numbers in parenthesis indicate discharge loss or sediment export from WMUs.

3.5% exceedance. This amount of ex-PPT would represent an input of 15% of the BC standing water volume at that stage.

The pattern of discharge through the primary outlet of BC was bidirectional, typically flowing into the unit at higher stages and out at lower stages, as described in Hupp et al. (2008, Figure 10). Discharge gain or loss in the bypassing channel, WFDC (−32 to 110 m^3/s), had a weak correlation with increasing stage ($R^2 = 0.43$). BC internal discharge losses did not correlate with discharge gains or losses in the WFDC ($R^2 = 0.09$) or the river ($R^2 = 0.05$).

3.4. Residence Time

Residence time of the ARB at lower stages was dominated by the volume of water in the river channel (Figures 5, 6a, and 6b). As stage increased, volume and amount of discharge increased, generally leading to a reduction in RT for most flow-through units. This resulted in a volume-weighted RT curve that started close to the unweighted curve. As volumes on the floodplain increased the weighted RT deviated from the unweighted RT, and moved back toward the unweighted curve as discharge increased in connected units and days-at-stage declined. The reduced duration of higher stages caused shorter RT in singular I/O units at high stages (Figure 6, Table S3 in Supporting Information S1).

The SML unit water volume was almost entirely represented by the Six Mile Lake channel (99%) that carried approximately 54% of the ARB discharge (USGS site #07381590, USGS, 2022). Because of its nearly complete connectivity (relative to volume), it had a very short RT. FL did not show a clear trend in RT (Figures 3 and 6e). This lack of a trend did not appear to be due to the hydrologic influences of FLFL on the unit. Removal of FLFL from the FL unit for RT analysis did not improve the correlation with BLR stage (with FLFL $R^2 = 0.19$, without $R^2 = 0.10$) but did increase the RT of FL (minus FLFL volume) by 4.2 d on average. The FL outlier point for RT at 3.66 m (Figure 6e) was not associated with a large PPT event or storm but followed a rapid decrease in river stage (LAIS, 2022; USGS, 2022). A rapid decrease in river stage relative to interior stage could cause a reduction of inflowing water due to reduced hydraulic gradients into the WMU. This hypothesis is supported by the high outflowing discharge relative to inflow as well as in comparison to other BLR stages. Most other units exhibited clear reducing trends in RT with increasing stage (Figure 6). At lower stages, exposed channel beds restricted flow, reducing connectivity within the BC unit. The reduction of inputs to BC resulted in long residence times at lower stages (Figure 6d).

Poorly connected units, CS and AD, exhibited increasing RT as stage increased. These units had relatively low volumes of water contained within channels at lower stages. AD also had channel bed elevations that prevented inflow into large portions of the unit during lower stages. The increase in RT with stage may be a result of

incorrect assumptions about the flow patterns into those units. Flow reversals in input channels may occur (as seen in well-connected units), or possibly their RT may be better represented as a nonflowing and singular I/O unit.

Channel bed elevation restrictions to flow were common to most of the singular I/O channel units (W, LL, and CI). These singular I/O units act as lakes and their residence times, dictated by the hydrograph of the AR, resulted in residence times up to 231 d, except where physical blockages to drainage were present (Figures 4 and 6).

3.5. Dissolved Oxygen

Dissolved oxygen in FL declined with RT at 3.7 m stage ($F_{1,203} = 8.02$, $P < 0.01$) in the best fitting GLM (identity link, normal distribution, and Pearson X^2/degree of freedom = 1.28, RMS = 1.1, and MAE = 0.87), whereas RT-DO relationships at 4.0 and 4.7 m were not statistically significant. The model indicated that when flooding exceeded 3.7 m per day, dissolved DO declined by −0.21 mg/l per day ($t = -2.83$, $P < 0.01$; Figure 8). While some increasing trend in DO may seem apparent above the 1.5-year flood stage (4.8 m, Figure 8), insufficient sampling dates existed to be statistically significant ($P = 0.13$).

Trends of declining DO concentrations with increasing days-at-stage indicates that RT in FL is long enough for biotic and chemical oxygen demand to strip DO from the water column as temperatures rise above 20°C. A contributing factor in this WMU may be the large areas of swamp within FL that are isolated from the through-flow of the unit (Allen et al., 2008; Hupp et al., 2019); although the unit as a whole is well-connected to source waters, large areas may act as forested, backwater lakes. While oxygenated water increases floodplain DO during rising stages, high oxygen demand on the floodplain, as well as respiring organisms and decomposing aquatic vegetation in open water, deplete DO across large areas of the lower ARB as stages decrease (Colon-Gaud et al., 2004; Kaller et al., 2015; Pasco et al., 2015).

3.6. Sediment Trapping

Sediment trapping was substantial during the higher stage events, with FL capturing a maximum of 25 Gg (Gg)/day, GIWW 11 Gg/day, and BC 3.3 Gg/day (Table 4). This trapped mass represented 12% of the suspended sediment load in the river on the days sampled, relative to the USGS river sampling (8.7% FL + GIWW, 3.4% BC; Figure 9). Sediment trapping in both FL and BC showed a strong correlation with the gain or loss of discharge within the unit (FL $p = 0.02$, BC $p = 0.03$; Figure 9). FL sediment storage also showed a strong correlation with SSC ($p = 0.01$) but was not significantly correlated with RT, inflow, water volume of the unit, or stage (Figure 9a). In contrast, sediment trapping in BC was not correlated with SSC ($R^2 = 0.50$ and $p = 0.55$) but was correlated with the water volume of the unit ($p = 0.01$) and RT ($p = 0.02$, Figure 9b).

At stages below 2 m at BLR, FL, and BC either exported or did not store sediment. At the lowest sampled stage, sediment exported from FL + GIWW (2.0 Gg/day) represented 22% of the sediment exported from the ARB (6.6 Gg/day). Examination of FLFL indicated it to be a large source of the exported sediment from FL, although all portions of the FL + GIWW exported much more sediment than input at those low stages (Figure 10, Table 4). Sediment export and trapping in FL and BC ranged from −266% to 91% and from −263% to 99% efficiency, respectively. The extreme sediment TE of BC was likely facilitated by discharge losses within the unit of up to 96% of incoming discharge. Similarly, the highest sediment TE for FL occurred during a sampling mission with 43% discharge loss, which may have been influenced by a wind seiche in the Gulf of Mexico recorded at the MC streamgage (Table 1, streamgage 17) and others along the Gulf Coast. Other FL missions within a ±0.15 m range of the stage at maximum TE (3.81 m) averaged 68% efficiency (Table 4).

4. Discussion

4.1. Residence Time and Discharge

Although consideration of a river/floodplain system's total RT is important, the concentration of discharge in the river channel masks the influence and processes of floodplain complexity. In our study, we observed four categories of floodplain hydrologic connectivity in the ARB (Figure 11). Poorly connected WMUs received inflows through created access channels that were not estimated to be able to supply a commensurate increase of inflow

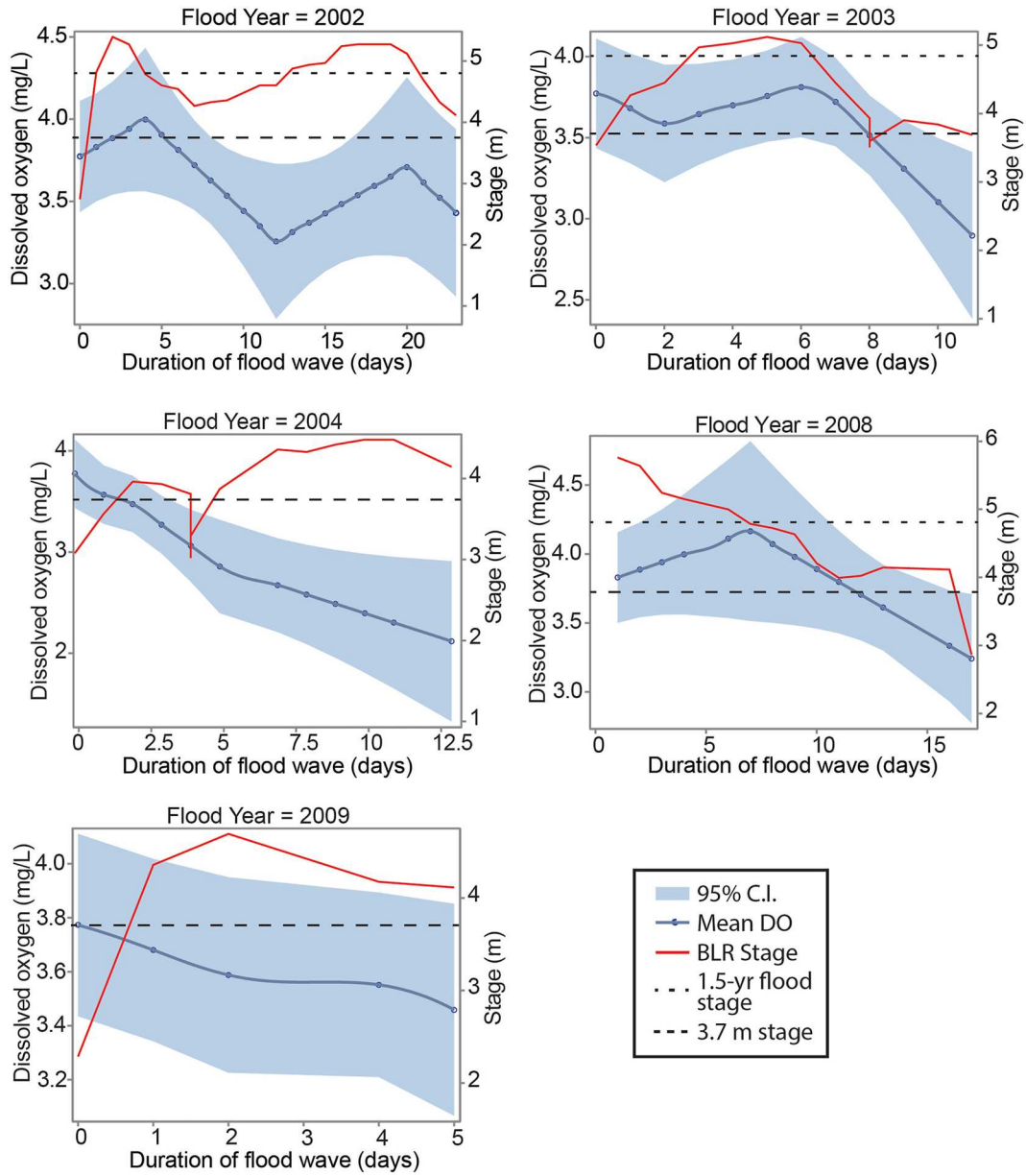

Figure 8. Relationship in FL of dissolved oxygen (mg/L–dotted line) with residence time (days) superposed with stage (m-solid line). Bands represent 95% confidence intervals. Short-dashed lines indicate the 1.5-year flood stage (4.8 m), long-dashed lines indicate a stage of 3.7 m of the Atchafalaya River at Butte la Rose.

as the increasing water volumes with stage (Figures 5 and 7). This limited supply led to increasing residence times as stage increased (Figure 6). I/O WMUs, whose hydrology was dominated by backwater river water inflow and outflow from a single channel, had a range of residence times dictated by the river flood wave (up to 231 d, Figure 6). Well-connected WMUs showed substantial inflows. FL had substantial inflows at all stages, while BC had very low inflow at low stages that substantially increased as stages and water volumes increased. One WMU exhibited almost complete connectivity with half of the AR flow, with the majority of that WMU's water volume in its channel (Figure 11). These four categories (poorly connected, I/O, well connected, and throughflow) over-simplify the structural complexity of each WMU on the floodplain.

Typically, discharge crossing the floodplain is considerably lower than the discharge in the river channel (Bonnet et al., 2008; Richey et al., 1989; Song et al., 2014). Even though the discharge crossing the ARB floodplain was a relatively small percentage of the AR, discharge across the floodplain exceeded 500 m^3/s at median stage and

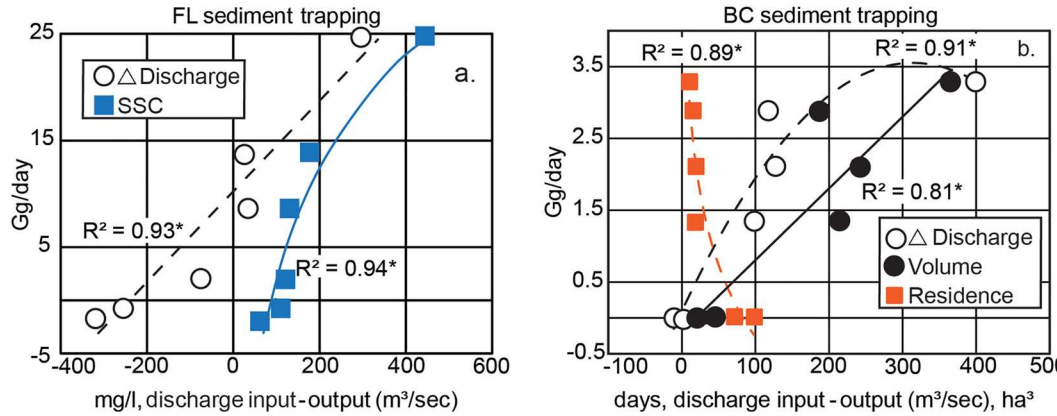

Figure 9. Significant factors relating to sediment trapping for FL (a) and BC (b). Δ discharge = input—output. * indicates $p < 0.05$. FL sediment trapping correlated with discharge and incoming suspended sediment concentrations (SSC). BC sediment trapping correlated with discharge, interior volume, and residence time.

up to 2,200 m^3/s during a 1.5-year flood, not including bypassing channels, and as a percentage was slightly greater than in other studied river floodplain systems (Rudorff et al., 2014a; Song et al., 2014). Comparatively, this median floodplain discharge was approximately equivalent to the entire median discharges of the Klamath (CA) or Connecticut (CT) Rivers (USGS, 2007; USGS, 2014b).

The volumes of the mean and 10% exceedance ex-PPT relative to the standing volume of the WMUs could be substantial at lower stages where most water volume was contained within the floodplain channels and stages below channel blockages on I/O WMUs (Table S4 in Supporting Information S1). Indeed, ex-PPT was likely the only source of water for several WMUs when their channel bottoms were above the river stage. Our volume calculations for ex-PPT volume contributions assumed 100% runoff, which is unlikely on a forested natural sediment surface. Actual runoff could range from 0% to 90%, depending on the antecedent conditions and the PPT event characteristics (Zhang et al., 2006). The only synoptic discharge sampling mission that followed a low exceedance ex-PPT event (BC, 1.68 m BLR, and 3.5% exceedance) resulted in a modest 11 m^3/s gain in output flow from the WMU (Table 3) even though the ex-PPT volume totaled 15% of the standing volume of the unit.

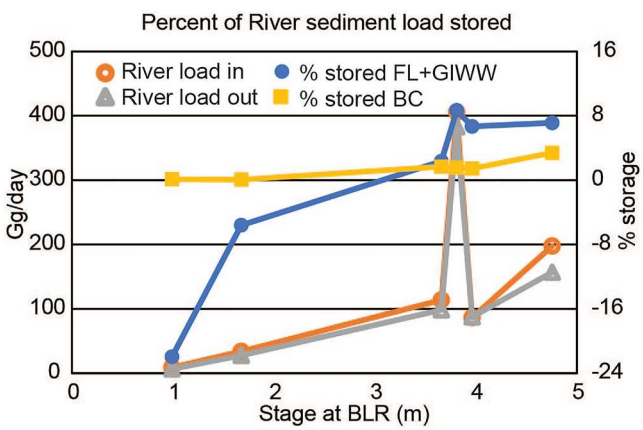

Figure 10. River sediment load in gigagrams (Gg)/day entering and leaving the Atchafalaya River Basin on the 2010–2011 dates that Flat Lake (FL) was sampled, and the percentage of incoming river sediment load stored in the FL water management units (WMU) and Gulf Intracoastal Waterway (GIWW) as sampled. Buffalo Cove (BC) sediment trapping was determined by sediment trapping efficiency at those stages relative to suspended sediment concentrations at the USGS Atchafalaya River at Simmesport (USGS site #07381490, USGS, 2022) on those dates.

The timing of sampling on the hydrograph (i.e., rising or falling limb) did introduce variation in the volume of the WMUs. We sought to minimize these variations by averaging the means of rising and falling stages at BLR with the streamgages used to calculate the WMU surfaces. However, in one synoptic discharge measurement set (FL, 3.66 m BLR), higher water inside the WMU relative to dropping river levels may have reduced the inflow to the unit while increasing the outflow (Table 3). Seiches in the Gulf of Mexico also could have affected outflow from FL (3.81 m BLR). Increased water levels in the Gulf resulted in increased stages at MC, where FL drains into the river. High water levels in the receiving waterbodies reduced the ability of the WMU to drain for the duration of the seiche (Lamb et al., 2012), even at relatively high river stages.

Our study differs from previous modeling studies of the ARB. These modeling efforts were designed to measure the changes in water levels and storage in relation to floodplain topography and flow resistance (Bell et al., 2018; Jung et al., 2012; Moffatt & Nichol, 2012). These models are useful for their intended purpose; however, their focus is generally on the entire ARB and not on flow patterns within WMUs. These models, at least for their published portions, were designed around discharges that exceeded the 1.5-year flood. For example, Bell et al. (2018) considered the flood of 2008 from April 1 to June 1. During this period, water levels were greater than 3.5 m in the BC

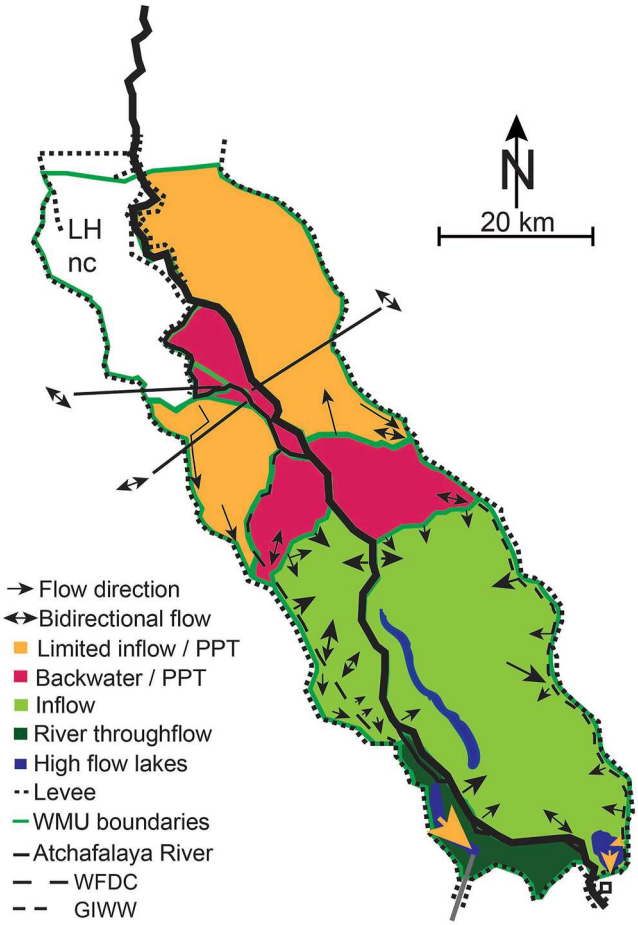

Figure 11. Dominant hydrology of water management units (WMUs) of the Atchafalaya River Basin, including flow directions and relative magnitudes of major flow inputs and outputs. Poorly connected WMUs had hydrology dominated by limited inflow and precipitation (PPT). I/O WMUs had hydrology dominated by backwater and PPT. Well-connected units were dominated by inflow. Six Mile Lake (SML) was dominated by river throughflow. Lake Henderson was not considered (nc). WFDC=West Freshwater Distribution Canal, and GIWW = Gulf Intracoastal Waterway. Base map modified from USACE (1982).

WMU. Our highest stage considered in the BC WMU was 3.1 m NAVD88 (Table S1 in Supporting Information S1).

4.2. Dissolved Oxygen

Given the volume of discharge across the ARB floodplain, it may be counter-intuitive that high DO (>3.0 mg/l) conditions were not sustained throughout the FL WMU as water temperatures rose above 20°C. As expected, increases in the duration of the investigated flood waves led to longer residence times, which caused DO to decline substantially, resulting in widespread hypoxia that typically characterizes the latter stages of the annual ARB flood pulse (Kaller et al., 2011; Pasco et al., 2015; Sabo et al., 1999). In context of the large spatial area of inundation and the minimal gradient across the ARB floodplain, water and wind velocities were insufficient to aerate the water column below the surface layer. Algae blooms are not common in the ARB due to high turbidities (Hern et al., 1980), so their effects on DO were not considered to be the major cause of hypoxia. However, autochthonous and allochthonous organic matter (detritus) are a major input to this system, and decomposition of particulate and dissolved organic carbon presents substantial demands on DO concentrations (Hupp et al., 2019; Kaller et al., 2015; Pasco et al., 2015).

Development of hypoxic conditions from decomposition of organic carbon sources during floodplain inundation in the ARB is a common feature of tropical and subtropical floodplains throughout the world (Hamilton et al., 1997; Irvine et al., 2011; Mosley et al., 2021; Richey et al., 1988; Wong et al., 2010; Zurbrügg et al., 2012), resulting in significant effects on biotic composition and function (e.g., fish behavior, survival, and morphology; Petry et al., 2013; Saint-Paul & Soares, 1987; Scarabotti et al., 2011; da Silva et al., 2010; Townsend & Edwards, 2003). The magnitude and timing of the flood pulse can have substantial impacts on water quality in the source river (Hamilton et al., 1997; Zurbrügg et al., 2012), and anthropogenic alterations of flood pulse characteristics (e.g., from dams, levees, channelization; Mosley et al., 2021) can significantly alter the physicochemical nature of the river-floodplain relationship. Understanding flood pulse effects on floodplain water quality, particularly DO, is a central part of efforts to develop flood management strategies to reduce biotic impacts (Howitt et al., 2007; Whitworth & Baldwin, 2016).

It is likely that backwater portions of the unit that were less hydrologically connected to flow (Allen et al., 2008; Hupp et al., 2019), with longer residence times, may have been contributing hypoxic water to better connected sampling locations as the duration of flooding increased. This contribution of hypoxic water likely increased as stages declined and floodplain waters drained (Jones et al., 2014; Kaller et al., 2015; Pasco et al., 2015). At stages of 4.0 m and above, the lack of a relationship with RT and DO may indicate that sufficient discharge and velocity resulted in greater aeration, which may have flushed some of the accumulated organic carbon out of the unit, reducing biological and sediment oxygen demands, or that turbulence and re-aeration from river inputs was sufficient to offset floodplain decomposition. Jones et al. (2014) observed similar conditions during a BLR stage of approximately 4.3 m NAVD88 where, as waters were rising, DO concentrations were reduced and dissolved organic carbon concentrations (DOC) were high. In our study, we observed a nonsignificant increasing trend of DO with stages above the 1.5-year flood (4.8 m NAVD88 BLR, Figure 8). As banks became totally inundated and hydrologic connections were increased well beyond our study's range to 6.7 m NAVD88, Jones et al. (2014) also found that DO increased and DOC was substantially reduced. Likewise, Ahearn et al. (2006) observed that portions of the Cosumnes River floodplain were not flushed during flood water inflows, contributing to localized hypoxia. Deoxygenation of water entering and remaining on the floodplain, particularly at elevated temperatures (i.e., >20 C), is a

common feature of the ARB and other well-studied floodplain systems in South America, Australia, and Asia (e.g., Hamilton et al., 1997; Irvine et al., 2011; Richey et al., 1988; Whitworth & Baldwin, 2016). Increasing water residence times at intermediate stages likely maintains high decomposition rates on the floodplain (if temperatures remain elevated), emphasizing the complex interactions among water temperature and the timing, magnitude, and duration of flooding, all of which ultimately determine floodplain and river oxygen dynamics.

4.3. Sediment Trapping

The mass of trapped sediment in the ARB was substantial. Deposition studies in the ARB (Hupp et al., 2008, 2019) indicate that, along with the associated particulate nutrients, up to 12.5 Tg of sediment and 690 Mg of organic carbon were deposited annually. If the mean concentration of particulate N and P (0.2% and 0.09%, USGS site #07381495) were extrapolated to the maximum daily sediment trapping measured in this study for the FL + GIWW and BC units (38 Gg/day), particulate nutrient trapping would equate to 76 Mg/day *N* and 34 Mg/day *P*. In comparison, the combined floodplains of the Chesapeake Bay watershed annually trap 5.3 teragrams (Tg) of total sediment, 16,000 Mg (Mg) of N and 5,300 Mg of P (Noe et al., 2022).

Although these calculated masses are quite large, they may not exceed the level of measurement and sampling error on the river. If sediment and nutrients loads were calculated from the river import and export alone, the confidence interval of measurement is ±5% for the input and ±5% for each of the two outputs. However, at very high discharge (19,000 m^3/s) when most banks were submerged and off-channel discharge exceeded channel discharge, nutrient reductions have been shown to be substantial (Scott et al., 2014).

Measured losses of discharge and gains in the well-connected units were considerable in volume, and it was likely that other units also lost or gained water. A likely sink or source of water may be the underlying alluvial aquifer (Helton et al., 2014). This study found no correlation of these losses with river discharge losses or gains. Similarly to ARB sediment and nutrient deposition, the water losses measured in this study were less than the river discharge measurement uncertainty and could not be accounted for using a simple input/output water balance for the whole system.

Sediment trapping was limited by inflowing discharge volumes in I/O units and poorly connected units. However, field observations indicate that where sediment is introduced to the interior, deposition is heavy and spatially concentrated to the area where flow encounters the standing pool of the WMU and is no longer contained within a channel. This interface of inflow and low-velocity water causes a prograding delta into the relict channel or lake (Kroes & Kraemer, 2013). In many stream/floodplain ecosystems, flow is largely distributed across the floodplain, and high flow velocities distribute sediment over large areas rather than in prograding deltas (McMillan & Noe, 2017). However, in the ARB, high levee deposits were formed during a period of rapid channel modification and evolution under a flow regime that no longer exists. These deposits have restricted the locations and manner that water flows into these WMUs. Sheet flow from the river or primary distributaries into WMUs has been almost eliminated during a 1.5-year flood (Kroes et al., 2022). These conditions are not unique to the ARB and have been observed on the Selenga River Delta lakes (Russia; Pietron et al., 2018) and other floodplain lakes similar to oxbows (Rowland et al., 2005).

4.4. Management Considerations

Large areas within the ARB could experience improved water quality by throughflow introduction and/or enhancement of existing flow paths. Poorly connected WMUs comprised 28% (613 km^2) of our study area. I/O WMUs comprised 15% (330 km^2) of our study area prior to 2015 (Figure 11). I/O units are functionally equivalent to a forested oxbow lake. Since 2015, additional inputs have been added to BB (LADNR, 2016). While post construction monitoring has not been completed, imagery from Sentinel satellites shows a broad distribution of turbid water through the swamp (10 April 2021, Sinergise Ltd, 2022). However, this study's findings show that simply increasing throughflow does not necessarily result in the elimination of hypoxia, as might be anticipated.

Many obstructions to flow exist on this floodplain, forming pockets of water with high residence times away from the WMU flow paths that can result in overall reductions in DO as flood durations become extended and water temperatures rise (Baustian et al., 2019). This study examined water RT in large-scale, considering the WMUs as monolithic units and overlooked these longer RT inclusions. A large-scale deuterium study may improve the

understanding of the percentages and RT of isolated waters in each WMU, and such a study could benefit from the WMU water volumes and flow rates presented here.

Large areas of ARB floodplain are increasingly becoming permanently inundated as the combined effects of subsidence and sea level rise increase low water levels (Kroes et al., 2022). Increasing the area of floodplain that is permanently inundated increases the storage of organic carbon on the floodplain, which can result in increased oxygen demands for the water column (Kaller et al., 2015). To reduce nonflowing inclusions of the WMUs, flow could be increased at upstream locations and spoil banks could be reduced in relation to the WMU's stage exceedance curves (Kroes et al., 2022).

5. Conclusions

The ARB captured large masses of sediment [(and likely the associated particulate N and P (12% of daily ARB load)] at high discharge and exported sediment at low discharge (22% of daily ARB load). Although several factors influenced sediment trapping on the floodplain, hydrologic connectivity appeared to be most important for the major WMUs in the lower ARB, with water entering and leaving the units by surface water and possibly by groundwater. Water passing into the WMUs ranged from 85 to 2,200 m^3/s and residence times were long (6 to 230 days), which provided ample opportunity for high sediment trapping efficiencies and dissolved nutrient denitrification and adsorption. However, extended flood durations also resulted in widespread hypoxic conditions as water temperatures increased toward the end of the flood wave, likely remobilizing nutrient storage (Welch et al., 2014).

The percentage of sediment trapping and losses to groundwater were not consistently represented by measurements of the river, largely because discharge ratings have at best a ±5% accuracy. There are three discharge sites that measure the water and sediment balance of the ARB, indicating up to a ±15% range for discharge and load estimates. Future studies of sediment and nutrient processing on the floodplain could focus on primary tributary and distributary channels within the floodplains to gain better resolution of floodplain functions and processes.

The ARB differs from many streams/rivers in that water leaving the channel has one floodplain interaction prior to leaving the system. Consequently, if 10% of the river discharge crosses the floodplain during the annual flood pulse, only this volume is subject to floodplain processes during that period. In contrast, other systems can exhibit more frequent water exchanges between the floodplain and river before exiting the system (Amoros & Bornette, 2002; Czuba et al., 2019; Junk et al., 1989). In these systems, 10% of river discharge may cross from the river to the floodplain and back many times, increasing the volume of water available for floodplain processing (Malard et al., 2002; Tockner et al., 1999). Nevertheless, the volume and mass of water, sediment, and nutrients that cross and become trapped on the ARB floodplain is extremely large. If annualized, nutrient trapping in the ARB would be comparable to the nutrient trapping of all the Chesapeake Bay watershed floodplains. As such, this is notable at the continental scale.

Floodplains are not a homogenous surface, large floodplains like the Amazon through small streams with beaver ponds exhibit structural complexity on their floodplains (Lewin & Ashworth, 2014; Park & Latrubesse, 2017; Wohl et al., 2021). On medium to large alluvial floodplains like the Fly River, Papua New Guinea, flows across the floodplain form prograding channels (Day et al., 2008) that eventually create poorly connected pockets of water during flooding. On many large and small floodplains, structural heterogeneity like elevated roadways, secondary levees, or natural/biogenic features on the floodplains may be limiting the flow exchange through those floodplains, as they do on the ARB floodplain. Many large floodplains, like the Mekong River floodplain, are experiencing active construction (Fujii et al., 2003) that will continue to increase structural complexity and heterogeneity of flow.

Structural complexity, both geomorphic and vegetative, leads to preferential flow paths across the floodplain (Allen et al., 2008; Kroes & Hupp, 2010; Kroes & Kraemer, 2013; Kroes et al., 2015; Molliex et al., 2019). Within each of the studied ARB WMU's there existed a spectrum of hydrologic connectivity that likely also ranged from nonflowing backwater to full channel connectivity (Allen et al., 2008; Hupp et al., 2019). These types of differences in temporal and spatial distances to preferential flow paths significantly alter the chemistry of the water (Hupp et al., 2019; Jones et al., 2014). Many rivers on the Coastal Plains have long flood waves that may last weeks, months, or have permanent surface water on the floodplain. Using river discharge to estimate the floodplain water residence times alone could substantially underestimate water residence times and nutrient

processing on the floodplain, while not assessing floodplain structural obstacles to flow could result in reduced areas of restoration impact. Oversimplification of RT calculations and failure to identify structural obstructions could undermine the benefits and longevity of floodplain restorations.

Data Availability Statement

The data on which this article is based are available from the following cited references and URLs: Kaller, M. (2022), Kroes, D.E. (2022), Louisiana Agriclimatic Information System (LAIS, 2022), U.S. Army Corps of Engineers (USACE, 2012), U.S. Army Corps of Engineers (USACE, 2022b), U.S. Geological Survey (USGS, 2012), U.S. Geological Survey (USGS, 2014a), and U.S. Geological Survey (USGS, 2022).

Acknowledgments
Thanks to all the people who have worked on these projects over the decades. This study was funded in part by cooperative agreements with the United States Army Corps of Engineers MVN, the Louisiana Department of Natural Resources Atchafalaya Basin Program, Audubon Louisiana, and the U.S. Department of Agriculture National Institute of Food and Agriculture, Hatch project accession number 1013004 and McIntire-Stennis Cooperative Forestry Program as Project Number LAB-94335. This manuscript was approved for publication by the Director of the Louisiana Agricultural Experiment Station as MS 2022-241-37273. Any use of trade, firm, or product names is for descriptive purposes only and does not imply endorsement by the U.S. Government.

References

Ahearn, D., Viers, J. H., Mount, J. F., & Dahlgren, R. A. (2006). Priming the productivity pump: Flood pulse driven trends in suspended algal biomass distribution across a restored floodplain. *Freshwater Biology*, *51*(8), 1417–1433. https://doi.org/10.1111/j.1365-2427.2006.01580.x

Allen, Y. C., Constant, G. C., & Couvillion, B. R. (2008). *Preliminary classification of water areas within the Atchafalaya Basin Floodway system by using Landsat imagery*. U.S. Geological Survey, Open File Report, 2008-1320.

Amoros, C., & Bornette, G. (2002). Connectivity and biocomplexity in waterbodies of riverine floodplains. *Freshwater Biology*, *47*(4), 761–776. https://doi.org/10.1046/j.1365-2427.2002.00905.x

Associate Press (AP). (2020). Louisiana joins two lawsuits challenging how Bonnet Carre Spillway is operated. Retrieved from https://www.nola.com/news/environment/article_5492ff02-b0a7-11ea-97ab-3f1a811f6bdb.html

Baustian, J. J., Piazza, B. P., & Bergan, J. F. (2019). Hydrologic connectivity and backswamp water quality during a flood in the Atchafalaya ARB, USA. *River Research and Applications*, *35*(4), 430–435. https://doi.org/10.1002/rra.3417

Becker, M., Papa, F., Frappart, F., Alsdorf, D., Calmant, S., Santos da Silva, J., et al. (2018). Satellite-based estimates of surface water dynamics in the Congo River Basin. International. *Journal of Applied Earth Observation and Geoinformation*, *66*, 196–209. https://doi.org/10.1016/j.jag.2017.11.015

Bell, G. L., Abraham, D. D., & Clifton, N. D. (2018). *Hydrodynamics in the morganza Floodway and Atchafalaya Basin, report 2: Phase 2*. US Army Corps of Engineers MRG&P Report No. 26,

Bonnet, M. P., Barroux, G., Martinez, J. M., Seyler, F., Turcq, P. M., Cochonneau, G., et al. (2008). Floodplain hydrology in an Amazon floodplain lake (Lago Grande de Curuaí). *Journal of Hydrology*, *349*(1–2), 18–30. https://doi.org/10.1016/j.jhydrol.2007.10.055

Bryant-Mason, A., Xu, Y. J., & Altabet, M. (2013a). Isotopic signature of nitrate in river waters of the lower Mississippi and its distributary, the Atchafalaya. *Hydrological Processes*, *27*(19), 2840–2850. https://doi.org/10.1002/hyp.9420

Bryant-Mason, A., Xu, Y. J., & Altabet, M. A. (2013b). Limited capacity of river corridor wetlands to remove nitrate: A case study on the Atchafalaya River basin during the 2011 Mississippi river flooding. *Water Resources Research*, *49*(1), 283–290. https://doi.org/10.1029/2012WR012185

Colon-Gaud, J. C., Kelso, W. E., & Rutherford, D. A. (2004). Spatial distribution of macroinvertebrates inhabiting hydrilla and coontail beds in the Atchafalaya Basin, Louisiana. *Journal of Aquatic Plant Management*, *42*, 85–90.

Czuba, J. A., David, S. R., Edmonds, D. A., & Ward, A. S. (2019). Dynamics of surface-water connectivity in a low-gradient meandering river floodplain. *Water Resources Research*, *55*(3), 1849–1870. https://doi.org/10.1029/2018WR023527

da Silva, H. P., Petry, A. C., & da Silva, C. J. (2010). Fish communities of the pantanal wetland in Brazil: Evaluating the effects of the upper Paraguay River flood pulse on baía caiçara fish fauna. *Aquatic Ecology*, *44*(1), 275–288. https://doi.org/10.1007/s10452-009-9289-9

Davis, B. E. (2005). *A guide to the proper selection and use of federally approved sediment and water quality samplers*. U.S. Geological Survey Open-file Report 2005-1087.

Day, G., Dietrich, W. E., Rowland, J. C., & Marshall, A. (2008). The depositional web on the floodplain of the Fly River, Papua New Guinea. *Journal of Geophysical Research*, *113*(F1), F01S02. https://doi.org/10.1029/2006JF000622

Doble, R. C., Crosbie, R. S., Smerdon, B. D., Peeters, L., & Cook, F. J. (2012). Groundwater recharge from overbank floods. *Water Resources Research*, *48*(9), W09522. https://doi.org/10.1029/2011WR011441

Ensign, S. H., Noe, G. B., & Hupp, C. R. (2014). Linking channel hydrology with riparian wetland accretion in tidal rivers. *Journal of Geophysical Research: Earth Surface*, *119*(1), 28–44. https://doi.org/10.1002/2013jf002737

Environmental Systems Research Institute (ESRI). (2019). ArcPro release 2.3.

Fatras, C., Parrens, M., Peña Luque, S., & Al Bitar, A. (2021). Hydrological dynamics of the Congo Basin from water surfaces based on L-band microwave. *Water Resources Research*, *57*(2), e2020WR027259. https://doi.org/10.1029/2020wr027259

Fontenot, R. L. (2004). An evaluation of reference evapotranspiration models in Louisiana. LSU master's thesis 4253. Retrieved from https://digitalcommons.lsu.edu/gradschool_theses/4253/

Fujii, H., Garsdal, H., Ward, P., Ishii, M., Morishita, K., & Boivin, T. (2003). Hydrological roles of the Cambodian floodplain of the Mekong River. *International Journal of River Basin Management*, *1*(3), 253–266. https://doi.org/10.1080/15715124.2003.9635211

Google Earth. (2019). Atchafalaya River basin imagery 2001-2019. N 30:08 W 91:29. 9.

Guy, H. P., & Norman, V. W. (1970). Field methods for measurement of fluvial sediment. In *U.S. Geological survey techniques of water-resources investigations* (Vol. 3). U.S. Geological Survey.

Hamilton, S. K., Sipper, S. J., Calheiros, D. F., & Melack, J. M. (1997). An anoxic event and other biogeochemical effects of the Pantanal wetland on the Paraguay River. *Limnology & Oceanography*, *42*(2), 257–272. https://doi.org/10.4319/lo.1997.42.2.0257

Heath, E. H., Brown, G. L., Little, C. D., Pratt, T. C., Ratcliff, J. J., Abraham, D. D., et al. (2015). *Old River Control complex sedimentation investigation*. US Army Corps of Engineers. USACE ERDC/CHL TR-15-8.

Helton, A. M., Poole, G. C., Payn, R. A., Izurieta, C., & Stanford, J. A. (2014). Relative influences of the river channel, floodplain surface, and alluvial aquifer on simulated hydrologic residence time in a montane river floodplain. *Geomorphology*, *205*, 17–26. https://doi.org/10.1016/j.geomorph.2012.01.004

Hern, S. C., Lambou, V. W., & Butch, J. R. (1980). *Descriptive water quality for the Atchafalaya Basin, Louisiana, volume 1* (p. 168). U.S. Environmental Protection Agency. EPA-600/4-80-014.

Howitt, J. A., Baldwin, D. S., Rees, G. N., & Williams, J. L. (2007). Modelling blackwater: Predicting water quality during flooding of lowland river forests. *Ecological Modelling*, *203*(3–4), 229–242. https://doi.org/10.1016/j.ecolmodel.2006.11.017

Hupp, C. R., Demas, C. R., Kroes, D. E., Day, R. H., & Doyle, T. W. (2008). Recent sedimentation patterns within the central Atchafalaya Basin, Louisiana. *Wetlands*, *28*(1), 125–140. https://doi.org/10.1672/06-132.1

Hupp, C. R., Kroes, D. E., Noe, G. B., Schenk, E. R., & Day, R. H. (2019). Sediment trapping and carbon sequestration in floodplains of the lower Atchafalaya Basin, LA: Allochthonous versus autochthonous carbon sources. *Journal of Geophysical Research: Biogeosciences*, *124*(3), 663–677. https://doi.org/10.1029/2018jg004533

Hupp, C. R., Schenk, E. R., Kroes, D. E., Willard, D. A., Townsend, P. A., & Peet, R. K. (2015). Patterns of floodplain sediment deposition along the regulated lower Roanoke River, North Carolina: Annual, decadal, centennial scales. *Geomorphology*, *228*, 666–680. https://doi.org/10.1016/j.geomorph.2014.10.023

Irvine, K. N., Richey, J. E., Holtgrieve, G. W., Sarkkula, J., & Sampson, M. (2011). Spatial and temporal variability of turbidity, dissolved oxygen, conductivity, temperature, and fluorescence in the lower Mekong River–Tonle Sap system identified using continuous monitoring. *International Journal of River Basin Management*, *9*(2), 151–168. https://doi.org/10.1080/15715124.2011.621430

Jones, C. N., Scott, D. T., Edwards, B. L., & Keim, R. F. (2014). Perirheic mixing and biogeochemical processing in flow-through and backwater floodplain wetlands. *Water Resources Research*, *50*(9), 7394–7405. https://doi.org/10.1002/2014WR015647

Joung, D., Guo, L., & Shiller, A. M. (2019). Role of the Atchafalaya River Basin in regulating export fluxes of dissolved organic carbon, nutrients, and trace elements to the Louisiana Shelf. *Journal of Hydrology X*, *2*, 100018. https://doi.org/10.1016/j.hydroa.2019.100018

Jung, H. C., Jasinski, M., Kim, J. W., Shum, C. K., Bates, P., Neal, J., & Alsdorf, D. (2012). Calibration of two-dimensional floodplain modeling in the central Atchafalaya Basin Floodway System using SAR interferometry. *Water Resources Research*, *48*(7). https://doi.org/10.1029/2012WR011951

Junk, W. J., Bayley, P. B., & Sparks, R. E. (1989). The flood pulse concept in river-floodplain systems. In D. P. Dodge (Ed.), *Proceedings of the lnternational large river symp. (LARS)* (Vol. 106, pp. 110–127). Canadian. Special Publications of Fisheries and Aquatic Sciences.

Kaller, M. D. (2022). *Dissolved oxygen concentrations of Flat Lake and East Grand Lake water management units of the Atchafalaya River basin*. U.S. Geological Survey data release. https://doi.org/10.5066/P9B43462

Kaller, M. D., Keim, R. F., Edwards, B. L., Harlan, A. R., Pasco, T., Kelso, W. E., & Rutherford, D. A. (2015). Aquatic vegetation mediates the relationship between hydrologic connectivity and water quality in a managed floodplain. *Hydrobiologia*, *760*(1), 29–41. https://doi.org/10.1007/s10750-015-2300-7

Kaller, M. D., Kelso, W. E., Halloran, B. T., & Rutherford, D. A. (2011). Effects of spatial scale on assessment of dissolved oxygen dynamics in the Atchafalaya River Basin, Louisiana. *Hydrobiologia*, *658*(1), 7–15. https://doi.org/10.1007/s10750-010-0470-x

Kroes, D. E. (2022). *Mean bed elevations of waterbodies on the Atchafalaya River floodplain*. U.S. Geological Survey data release. https://doi.org/10.5066/P94GULXE

Kroes, D. E., & Brinson, M. M. (2004). Occurrence of riverine wetlands on floodplains along a climatic gradient. *Wetlands*, *24*(1), 167–177. https://doi.org/10.1672/0277-5212(2004)024[0167:oorwof]2.0.co;2

Kroes, D. E., & Hupp, C. R. (2010). The effect of channelization on floodplain sediment deposition and subsidence along the Pocomoke River, Maryland. *Journal of the American Water Resources Association*, *46*(4), 686–699. https://doi.org/10.1111/j.1752-1688.2010.00440.x

Kroes, D. E., & Kraemer, T. F. (2013). Human-induced stream channel abandonment/capture and filling of floodplain channels within the Atchafalaya River Basin, Louisiana. *Geomorphology*, *201*, 148–156. https://doi.org/10.1016/j.geomorph.2013.06.016

Kroes, D. E., Demas, C. R., Allen, Y. A., Day, R. H., Roberts, S. W., & Varisco, J. (2022). Hydrologic modification and channel evolution degrades connectivity on the Atchafalaya River floodplain. *Earth Surface Processes and Landforms*, *47*(7), 1790–1807. https://doi.org/10.1002/esp.5347

Kroes, D. E., Hupp, C. R., & Noe, G. B. (2007). Sediment, nutrient, and vegetation trends along the tidal, forested Pocomoke River, Maryland. In W. H. Conner, T. W. Doyle, & K. W. Krauss (Eds.), *Ecology of tidal freshwater forested wetlands of the southeastern United States*. Springer.

Kroes, D. E., Schenk, E. R., Noe, G. B., & Benthem, A. J. (2015). Sediment and nutrient trapping as a result of a temporary Mississippi River floodplain restoration: The morganza spillway during the 2011 Mississippi River flood. *Ecological Engineering*, *82*, 91–102. https://doi.org/10.1016/j.ecoleng.2015.04.056

Lamb, M. P., Nittrouer, J. A., Mohrig, D., & Shaw, J. (2012). Backwater and river plume controls on scour upstream of river mouths: Implications for fluvio-deltaic morphodynamics. *Journal of Geophysical Research*, *117*(F1). https://doi.org/10.1029/2011jf002079

Leopold, L. B., Wolman, W. G., & Miller, J. P. (1964). *Fluvial processes in geomorphology*. W. H. Freeman and Company.

Lewin, J., & Ashworth, P. J. (2014). The negative relief of large river floodplains. *Earth-Science Reviews*, *129*, 1–23. https://doi.org/10.1016/j.earscirev.2013.10.014.10.014

Louisiana Agriclimatic Information System (LAIS). (2022). *Jeanerette, LA daily summary. 2001-11*. Louisiana State University Agricultural Center. Retrieved from https://app.lsuagcenter.com/weather-historical/reports.aspx?r=0

Louisiana Department of Natural Resources (LADNR). (2016). FY 2016 annual plan, Atchafalaya Basin program. LADNR. Retrieved from http://www.dnr.louisiana.gov/assets/OCM/ABP/2016_Plan/WEB_FINAL_ABP_2016_Plan.pdf

Malard, F., Tockner, K., Dole-Olivier, M. J., & Ward, J. (2002). A landscape perspective of surface–subsurface hydrological exchanges in river corridors. *Freshwater Biology*, *47*(4), 621–640. https://doi.org/10.1046/j.1365-2427.2002.00906.x

McMillan, S. K., & Noe, G. B. (2017). Increasing floodplain connectivity through urban stream restoration increases nutrient and sediment retention. *Ecological Engineering*, *108*, 284–295. https://doi.org/10.1016/j.ecoleng.2017.08.006issn:0925-8574

Mize, S. V., Murphy, J. C., Diehl, T. H., & Demcheck, D. K. (2018). Suspended-sediment concentrations and loads in the lower Mississippi and Atchafalaya Rivers decreased by half between 1980 and 2015. *Journal of Hydrobiology*, *564*, 1–11. https://doi.org/10.1016/j.jhydrol.2018.05.068

Moffatt and Nichol (2012). *Atchafalaya Basin Model, a hydrodynamic model of the Atchafalaya Basin, evaluating restoration alternatives, phase 2*. Baton Rouge.

Molliex, S., Kettner, A. J., Laurent, D., Droz, L., Marsset, T., Laraque, A., et al. (2019). Simulating sediment supply from the Congo watershed over the last 155 ka. *Quaternary Science Reviews*, *203*, 38–55. https://doi.org/10.1016/j.quascirev.2018.11.001

Mosley, L. M., Wallace, T., Rahman, J., Roberts, T., & Gibbs, M. (2021). An integrated model to predict and prevent hypoxia in floodplain-river systems. *Journal of Environmental Management*, *286*, 112213. https://doi.org/10.1016/j.jenvman.2021.112213

Natho, S., Tschikof, M., Bondar-Kunze, E., & Hein, T. (2020). Modeling the effect of enhanced lateral connectivity on nutrient retention capacity in large river floodplains: How much connected floodplain do we need? *Frontiers in Environmental Science*, *8*(74). https://doi.org/10.3389/fenvs.2020.00074

Noe, G. B., & Hupp, C. R. (2005). Carbon, nitrogen, and phosphorus accumulation in floodplains of Atlantic Coastal Plain rivers, USA. *Ecological Applications*, *15*(4), 1178–1190. https://doi.org/10.1890/04-1677

Noe, G. B., Hopkins, K. G., Claggett, P. R., Schenk, E. R., Metes, M. J., Ahmed, L., et al. (2022). Streambank and floodplain geomorphic change and contribution to watershed material budgets. *Environmental Research Letters*, *17*(6), 064015. https://doi.org/10.1088/1748-9326/ac6e47

Noe, G. B., Hupp, C. R., & Rybicki, N. R. (2013). Hydrogeomorphology influences soil nitrogen and phosphorus mineralization in floodplain wetlands. *Ecosystems*, *16*(1), 75–94. https://doi.org/10.1007/s10021-012-9597-0

Noe, G. B., Hupp, C. R., Bernhardt, C. E., & Krauss, K. W. (2016). Contemporary deposition and long-term accumulation of sediment and nutrients by tidal freshwater forested wetlands impacted by sea level rise. *Estuaries and Coasts*, *39*(4), 1006–1019. https://doi.org/10.1007/s12237-016-0066-4

Papa, F., Frappart, F., Malbeteau, Y., Shamsudduha, M., Vuruputur, V., Sekhar, M., et al. (2015). Satellite-derived surface and sub-surface water storage in the Ganges–Brahmaputra River basin. *Journal of Hydrology: Regional Studies*, *4*, 15–35. https://doi.org/10.1016/j.ejrh.2015.03.004

Park, E., & Latrubesse, E. M. (2017). The hydro-geomorphologic complexity of the lower Amazon River floodplain and hydrological connectivity assessed by remote sensing and field control. *Remote Sensing of Environment*, *198*, 321–332. https://doi.org/10.1016/j.rse.2017.06.021

Pasco, T. E., Kaller, M. D., Harlan, R., Kelso, W. E., Rutherford, D. A., & Roberts, S. (2015). Predicting floodplain hypoxia in the Atchafalaya River, Louisiana, USA, a large, regulated southern floodplain river system. *River Research and Applications*, *32*(5), 845–855. https://doi.org/10.1002/rra.2903

Petry, A. C., Abujanra, F., Gomes, L. C., Julio, H. F., Jr., & Agostinho, A. A. (2013). Effects of the interannual variations in the flood pulse mediated by hypoxia tolerance: The case of the fish assemblages in the upper paraná river floodplain. *Neotropical Ichthyology*, *11*(2), 413–424. https://doi.org/10.1590/s1679-62252013005000008

Piazza, B. P. (2014). *The Atchafalaya: History and ecology of an American wetland* (p. 305). Texas A&M University Press.

Pietroń, J., Nittrouer, J. A., Chalov, S. R., Dong, T., Kasimov, N., Shinkareva, G., & Jarsjö, J. (2018). Sedimentation patterns in the Selenga River delta under changing hydroclimatic conditions. *Hydrological Processes*, *32*(2), 278–292. https://doi.org/10.1002/hyp.11414

Rabalais, N., & Turner, E. (2019). Gulf of Mexico hypoxia: Past, present, and future. *Limnology and Oceanography Bulletin*, *28*(4), 117–124. https://doi.org/10.1002/lob.10351

Richey, J. E., Devol, A. H., Wofsy, S. C., Victoria, R., & Riberio, M. N. G. (1988). Biogenic gases and the oxidation and reduction of carbon in Amazon River and floodplain waters. *Limnology & Oceanography*, *33*(4), 551–561. https://doi.org/10.4319/lo.1988.33.4.0551

Richey, J. E., Mertes, L. A. K., Dunne, T., Victoria, R., Forsberg, B. R., Tancredi, A. C., & Oliveira, E. (1989). Source and routing of the Amazon River flood wave. *Global Biogeochemical Cycles*, *3*(3), 191–204. https://doi.org/10.1029/gb003i003p00191

Roley, S. S., Tank, J. L., Stephen, M. L., Johnson, L. T., Beaulieu, J. J., & Witter, J. D. (2012). Floodplain restoration enhances denitrification and reach-scale nitrogen removal in an agricultural stream. *Ecological Applications*, *22*(1), 281–297. https://doi.org/10.1890/11-0381.1

Rowland, J. C., Lepper, K., Dietrich, W. E., Wilson, C. J., & Sheldon, R. (2005). Tie channel sedimentation rates, oxbow formation age and channel migration rate from optically stimulated luminescence (OSL) analysis of floodplain deposits. *Earth Surface Processes and Landforms*, *30*(9), 1161–1179. https://doi.org/10.1002/esp.1268

Rudorff, C. M., Melack, J. M., & Bates, P. (2014a). Flooding dynamics on the lower Amazon floodplain: 2. Seasonal and interannual hydrological variability. *Water Resources Research*, *50*(1), 635–649. https://doi.org/10.1002/2013WR014714

Rudorff, C. M., Melack, J. M., & Bates, P. D. (2014b). Flooding dynamics on the lower Amazon floodplain: 1. Hydraulic controls on water elevation, inundation extent, and river-floodplain discharge. *Water Resources Research*, *50*, 619–634. https://doi.org/10.1002/2013WR014714

Sabo, M. J., Bryan, C. F., Kelso, W. E., & Rutherford, D. A. (1999). Hydrology and aquatic habitat characteristics of a riverine swamp: II. Hydrology and the occurrence of chronic hypoxia. *Regulated Rivers: Research & Management*, *15*(6), 525–544. https://doi.org/10.1002/(sici)1099-1646(199911/12)15:6<525::aid-rrr554>3.0.co;2-q

Saint-Paul, U., & Soares, G. M. (1987). Diurnal distribution and behavioral responses of fishes to extreme hypoxia in an Amazon floodplain lake. *Environmental Biology of Fishes*, *20*(2), 91–94. https://doi.org/10.1007/bf00005289

Samanta, A., Tripathy, G. R., & Das, R. (2019). Temporal variations in water chemistry of the (lower) Brahmaputra River: Implications to seasonality in mineral weathering. *Geochemistry, Geophysics, Geosystems*, *20*(6), 2769–2785. https://doi.org/10.1029/2018GC008047

Scarabotti, P. A., López, J. A., Ghirardi, R., & Parma, M. J. (2011). Morphological plasticity associated with environmental hypoxia in characiform fishes from neotropical floodplain lakes. *Environmental Biology of Fishes*, *92*(3), 391–402. https://doi.org/10.1007/s10641-011-9850-y

Schönbrunner, I. M., Preiner, S., & Hein, T. (2012). Impact of drying and re-flooding of sediment on phosphorus dynamics of river-floodplain systems. *Science of the Total Environment*, *432*(10), 329–337. https://doi.org/10.1016/j.scitotenv.2012.06.025

Scott, D. T., Keim, R. F., Jones, C. N., Edwards, B. L., & Kroes, D. E. (2014). Floodplain biogeochemical processing of floodwaters during the Mississippi River flood of 2011. *Journal of Geophysical Research*, *119*(4), 537–546. https://doi.org/10.1002/2013JG002477

Simpson, M. R. (2001). *Discharge measurements using a broad-band acoustic Doppler current profiler*. USGS -Open-File Report 01-1.

Sinergise Ltd. (2022). *Sentinel playground*. Sinergise Ltd. Retrieved from. https://apps.sentinel-hub.com/sentinel-playground. https://apps.sentinel-hub.com/sentinel-playground/?source=S2%26lat=30.169023970544924%26lng=-91.6204833984375%26zoom=12%26preset=1-NATURAL-COLOR%26layers=B01,B02,B03%26maxcc=100%26gain=1.5%26gamma=1.0%26time=2020-10-01%7C2021-04-10%26atmFilter=%26showDates=true

Song, S., Schmalz, B., & Fohrer, N. (2014). Simulation and comparison of stream power in-channel and on the floodplain in a German lowland area. *Journal of Hydrology and Hydromechanics*, *62*(2), 133–144. https://doi.org/10.2478/johh-2014-0018

Stackpoole, S., Sabo, R., Falcone, J., & Sprague, L. (2021). Long-term Mississippi river trends expose shifts in the river load response to watershed nutrient balances between 1975 and 2017. *Water Resources Research*, *57*(11), 1–19. https://doi.org/10.1029/2021wr030318

Sullivan, J. C., Wan, Y., & Willis, R. A. (2020). Modeling floodplain inundation, circulation, and residence time under changing tide and sea levels. *Estuaries and Coasts*, *43*(4), 693–707. https://doi.org/10.1007/s12237-020-00709-0

Tockner, K., Pennetzdorfer, D., Reiner, N., Schiemer, F., & Ward, J. V. (1999). Hydrological connectivity, and the exchange of organic matter and nutrients in a dynamic river-floodplain system (Danube, Austria). *Freshwater Biology*, *41*(3), 521–535. https://doi.org/10.1046/j.1365-2427.1999.00399.x

Townsend, S. A., & Edwards, C. A. (2003). A fish kill event, hypoxia and other limnological impacts associated with early wet season flow into a lake on the Mary River floodplain, tropical northern Australia. *Lakes and Reservoirs: Research and Management*, *8*(3–4), 169–176. https://doi.org/10.1111/j.1440-1770.2003.00222.x

Triantafillou, S. P. (2021). *The role of geomorphic variability on floodplain function: An analysis of sediment and phosphorus deposition* (Vol. 81). UVM College of Arts and Sciences College Honors Theses. Retrieved from https://scholarworks.uvm.edu/castheses/81

Turc, L. (1961). Evaluation des besoins en eau d'irrigation, evapotranspiration potentielle, formule climatique simplifee et mise a jour. (In French). *Annales Agronomiques*, *12*(1), 13–49.

U. S. Army Corps of Engineers (USACE). (1982). *Atchafalaya Basin Floodway System feasibility study—Main report and final environmental impact statement* (Vol. I, p. 358). U.S. Army Corps of Engineers.

U.S. Army Corps of Engineers (USACE). (2012). *Multibeam bathymetric data for the Atchafalaya River*. New Orleans. Retrieved from https://www.mvn.usace.army.mil/Missions/Engineering/Channel-Improvement-and-Stabilization-Program/2010MBAR/

U.S. Army Corps of Engineers (USACE). (2022a). Historical discharge of the Atchafalaya River at Simmesport. Retrieved from http://www2.mvn.usace.army.mil/cgi-bin/watercontrol.pl?03045

U.S. Army Corps of Engineers (USACE). (2022b). *Atchafalaya River and Floodway gages*. US Army Corps of Engineers. Retrieved from https://rivergages.mvr.usace.army.mil/WaterControl/new/layout.cfm

U.S. Climate Data. (2022). Lafayette, LA average annual temperature and precipitation. Retrieved from https://www.usclimatedata.com/climate/lafayette/louisiana/united-states/usla0261

U.S. Geological Survey (USGS). (1987). *Largest rivers of the United States*. Open File Report 87-242. Retrieved from https://pubs.usgs.gov/of/1987/ofr87-242/pdf/ofr87242.pdf

U.S. Geological Survey (USGS). (2007). *Water-resources data for the United States, water year 2006*. U.S. Geological Survey Water-Data Report WDR-US-2006, site 01184000, Retrieved from https://wdr.water.usgs.gov/wy2006/pdfs/01184000.2006.pdf?1599667449435

U.S. Geological Survey (USGS). (2011). *National Hydrography dataset (NHD)*. US Geological Survey. Retrieved from https://www.usgs.gov/core-sciencesystems/ngp/national-hydrography

U.S. Geological Survey (USGS). (2012). Atchafalaya Basin program NRIAS 20120914_update_Synoptic surveys. Retrieved from https://web.archive.org/web/20161203012744/https://abp.cr.usgs.gov/Library/Default.aspx?folder=35

U.S. Geological Survey (USGS). (2014a). 2010 U.S. Geological survey topographic Lidar: Atchafalaya basin, Louisiana. Retrieved from https://rockyweb.usgs.gov/vdelivery/Datasets/Staged/Elevation/LPC/Projects/LA_Atchafalaya2_2013/laz/

U.S. Geological Survey (USGS). (2014b). *Water-resources data for the United States, water year 2013*. U.S. Geological Survey Water-Data Report WDR-US-2013, site 11530500, Retrieved from http://wdr.water.usgs.gov/wy2013/pdfs/11530500.2013.pdf

U.S. Geological Survey (USGS). (2022). USGS water data for the Nation: U.S. Geological Survey. *National Water Information System database*. Retrieved from http://waterdata.usgs.gov/nwis/

van Meter, K. J., McLeod, M. M., Liu, J., Tenkouano, G. T., Hall, R. I., van Cappellen, P., & Basu, N. B. (2021). Beyond the mass balance: Watershed phosphorus legacies and the evolution of the current water quality policy challenge. *Water Resources Research*, *57*, 1–22.

Wang, H., Jia, X., Li, Y., & Peng, W. (2015). Selective deposition response to aeolian–fluvial sediment supply in the desert braided channel of the upper Yellow River, China. *Natural Hazards and Earth System Sciences*, *15*, 1955–1962. https://doi.org/10.5194/nhess-15-1955-2015

Welch, H. L., Coupe, R. H., & Aulenbach, B. T. (2014). *Concentrations and transport of suspended sediment, nutrients, and pesticides in the lower Mississippi-Atchafalaya River subbasin during the 2011 Mississippi River flood, April through July* (Scientific Investigations Report 2014–5100, p. 44). U.S. Geological Survey. https://doi.org/10.3133/sir20145100

Whitworth, K. L., & Baldwin, D. S. (2016). Improving our capacity to manage hypoxic blackwater events in lowland rivers: The Blackwater Risk Assessment Tool. *Ecological Modelling*, *320*, 292–298. https://doi.org/10.1016/j.ecolmodel.2015.10.001

Wohl, E., Castro, J., Cluer, B., Merritts, D., Powers, P., Staab, B., & Thorne, C. (2021). Rediscovering, reevaluating, and restoring lost river-wetland corridors. *Frontiers of Earth Science*, *9*. https://doi.org/10.3389/feart.2021.653623

Wong, V. N. L., Johnston, S. G., Bush, R. T., Sullivan, L. A., Clay, C., Burton, E. D., & Slavich, P. G. (2010). Spatial and temporal changes in estuarine water quality during a post-flood hypoxic event. *Estuarine, Coastal and Shelf Science*, *87*(1), 73–82. https://doi.org/10.1016/j.ecss.2009.12.015

Xu, Y. J. (2006). Organic nitrogen retention in the Atchafalaya River swamp. *Hydrobiologia*, *560*(1), 133–143. https://doi.org/10.1007/s10750-005-1171-8

Zhang, Q., Xu, C. Y., Becker, S., & Jiang, T. (2006). Sediment and runoff changes in the Yangtze River basin during past 50 years. *Journal of Hydrology*, *331*(3–4), 511–523. https://doi.org/10.1016/j.jhydrol.2006.05.036

Zurbrügg, R., Wamulume, J., Kamanga, R., Wehrli, B., & Senn, D. B. (2012). River-floodplain exchange and its effects on the fluvial oxygen regime in a large tropical river system (Kafue Flats, Zambia). *Journal of Geophysical Research*, *117*(G3), G03008. https://doi.org/10.1029/2011jg001853